1/22/79, 1238, Harbor Freeway underpass
HP 140, Whip, F 100 kHz, W 50 kHz, IF 3 kHz, ST 500 ms, A -20 dBm/0/+15 dB/NF

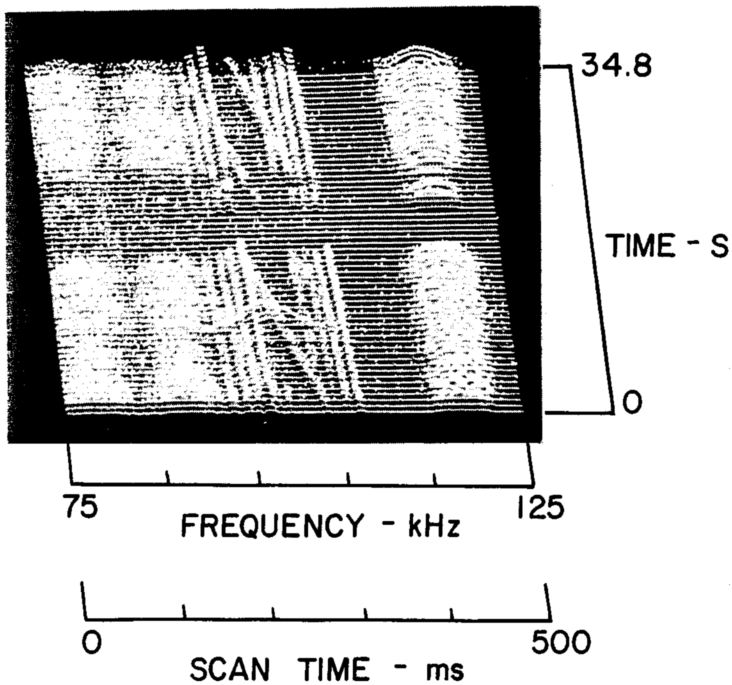

FIGURE 5-21. 3-AXIS VIEW, 1/22/79, 1238, HARBOR FREEWAY UNDERPASS

1/26/79, 0808, Harbor Freeway overpass impulse noise
HP 140, Whip, F 100 kHz, W 50 kHz, IF 3 kHz, ST 100 ms, A -20 dBm/0/+15 dB/NF

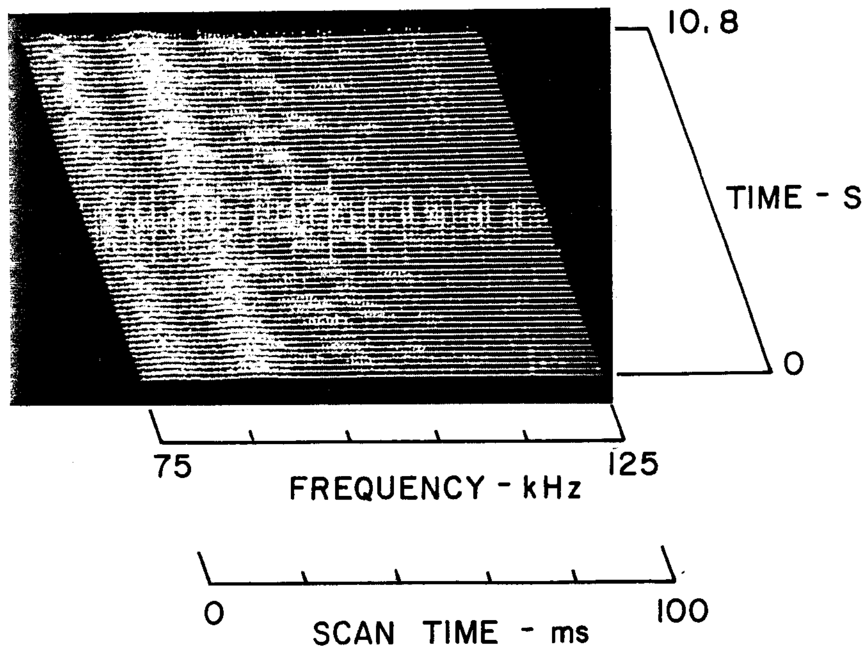

FIGURE 5-22. 3-AXIS VIEW, 1/26/79, 0808, HARBOR FREEWAY OVERPASS

5.3.8 Bursts of Power Line-Associated Noise

Bursts of noise were observed to be emanating from a high voltage utility transmission line crossing Rosecrans between Sepulveda and Vista Del Mar. These bursts are shown in Figure 5-23. Two bursts of noise can be seen in the upper portion of the view, each with a duration of about one second and spaced about 0.2 seconds apart. Downward in the view about 1.5 seconds further, another one-second burst of noise can be seen. About 0.4 seconds further down the view, two closely-spaced, very brief bursts occurred.

Signal structure during each burst had maximum and minimum energy at 8.3 ms intervals as shown by the slanting lines within each noise burst. Also, the maximum overall strength of the bursts peaked as the measurement van passed directly under the overhead transmission line.

Similar bursts of power line-associated noise have been observed in prior measurements at sites in Los Altos Hills, California, and Skaggs Island, California. The noise bursts have been observed to occur for periods up to a few hours and then to disappear for long periods of time. Their origin has not been determined, and possible source mechanisms have been the subject of much speculation. The on-off noise bursts remain a puzzle. While the Rosecrans transmission line provided a case where the source could probably have been tracked down with a small additional measurement effort, the time was not available for additional diagnostic effort.

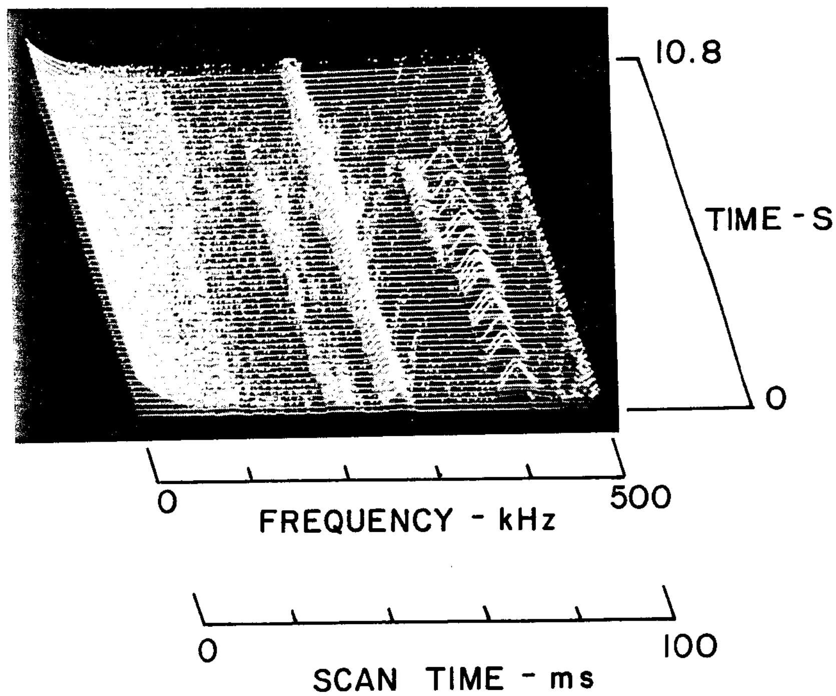

1/26/79, 1042, on Vista Del Mar passing under El Segundo power plant output lines
HP 140, Whip, F 250 kHz, W 500 kHz, IF 10 kHz, ST 100 ms, A -20 dBm/0/0/NF

FIGURE 5-24. 3-AXIS VIEW, 1/26/79, 1042, VISTA DEL MAR

1/26/79, 1038, on Vista Del Mar and passing under output lines El Segundo power plant
HP 140, Whip, F 2 MHz, W 50 kHz, IF 3 kHz, ST 100 ms, A -20 dBm/0/0/NF

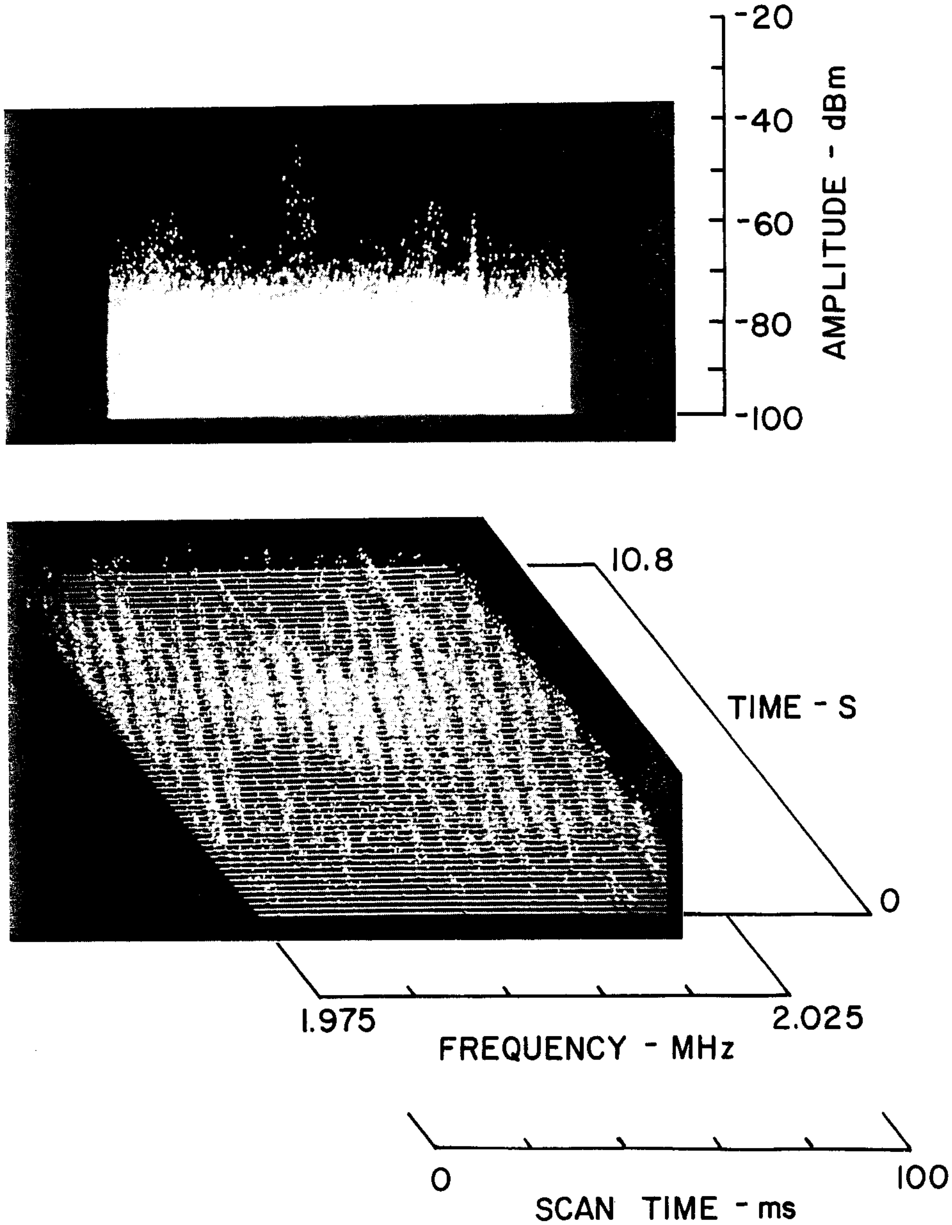

FIGURE 5-25. 3-AXIS VIEW, 1/26/79, 1038, VISTA DEL MAR

6. DISCUSSION

6.1 GENERAL COMMENTS

Results of the Phase II measurement period (January 22 through January 26, 1979) supplement those of the Phase I measurements described in Sections 3 and 4 (December 18 through December 22, 1978). While additional detail and data were collected, the results of this second measurement period were in general agreement with Phase I results. No significant differences in noise and RFI were found.

Slightly different measurement procedures were used in the first and second periods. During the first period the measurement van followed general route patterns for Loran-C receiver performance measurements, but the noise and RFI measurements were made at and around each site, as well as at many other locations where noise was observed. The noise and RFI measurements were of a diagnostic nature, with each measurement tailored to best define the noise being observed. The Phase II measurements were made primarily at specific sites and simultaneously with Loran-C receiver measurements. Supplementary measurements were made as time permitted.

Data from the fixed site measurements described in Section 5.2 and Appendix A have been organized and tabulated in formats convenient for two main objectives, which are:

1. To provide the reader with a valid and easy-to-interpret summary of radio noise and RFI in Los Angeles at and around the Loran-C transmission frequency of 100 kHz.
2. To provide a means to compare noise and RFI results at each site with the performance of Loran-C receivers.

6.2 FIXED SITE RESULTS

Noise and RFI measurements were made at 54 out of the 56 sites scheduled during the measurement period. Data were not obtained at two sites because of time required to clean an oscilloscope camera and to replace a fouled spark plug in the motor generator supplying 115 volt, 60 Hz power to the measurement van. A set of 3-axis views with standard measurement parameters was obtained at each of the 54 sites. The standard views were made with $F = 100$ kHz, $W = 50$ kHz, $IF = 3$ kHz, and $ST = 500$ ms. Data for sites 106-001 through 106-005 used the 18 dB preamplifier with the bandpass filter. At all remaining sites the 15 dB preamplifier was used without an RF filter.

Occasionally additional measurements were made with a larger scan width ($W = 100$ kHz) and/or at a faster scan speed ($ST = 100$ ms). The 3-axis views for these measurements follow the standard views, and their identification codes show the same site identification as the standard view with a different time of day and different measurement parameters.

Data for each site are provided in Appendix A. The 3-axis views in the appendix can be rapidly scanned to examine the variety of noise and CW signal states encountered.

Brief bursts of ignition noise were occasionally observed from vehicles passing the measurement van in an adjacent lane of traffic. Examples are shown in the data for sites 109-015, 109-016, 108-029, and 104-052. Most passing vehicles did not cause ignition impulses to appear in the data, and the examples provided might well represent the occasional super noise vehicle noted by Shepard, et al. (3) in higher frequency measurements.

An examination of the 3-axis views in Appendix A showed that all CW signals in the 75 to 125 kHz band appeared on five frequencies. The CW frequencies were approximately 80, 90, 100, 108, and 119 kHz. Precise frequency measurements were not made, and the accuracy of the above frequencies is about $\pm$ 1 kHz. The finding that all observed CW signals were only on a total of five frequencies considerably simplified data scaling and analysis tasks.

The level of each CW signal, each Loran-C signal, and the maximum peak pulse value of noise at 100 $\pm$ 10 kHz were scaled from the 3-axis views in Appendix A. The values of amplitude at the preamplifier input with all calibration factors incorporated are shown in Table 6-1. The columns of Table 6-1, from left to right, are:

Column 1	Site identification number (see Table 5-2)
2	Signal level in dBm of Loran-C Master Station located at
3	Signal level in dBm of Loran-C Station W located at
4	Signal level in dBm of Loran-C Station X located at
5	Signal level in dBm of Loran-C Station Y located at
6	Peak impulse level of noise in dBm in the 100 $\pm$ 10 kHz band
7	Signal level in dBm of CW signal at 80 kHz
8	Signal level in dBm of CW signal at 90 kHz
9	Signal level in dBm of CW signal at 100 kHz
10	Signal level in dBm of CW signal at 108 kHz
11	Signal level in dBm of CW signal at 119 kHz

The symbol < appears in columns 2 through 5 and it was used whenever the Loran-C signal was below the receiver noise level. The symbol - also appears in columns 2 through 5 and indicates times when signal level values could not be scaled from the 3-axis views because other signals prevented scaling. A 0 was used in columns 6 through 11 whenever noise or a CW signal was entirely absent from the 3-axis views.

The mean value of the peak measurements, $\overline{x}$, standard deviation, σ, and number of samples, N, are listed at the bottom of Table 6-1. The mean values and their standard deviations are provided because of the high interest in overall Loran-C receiving conditions. However, these values must be used with caution. The following listed factors must be considered when using the mean and standard deviation values.

1. The CW signals (except for 119 kHz) are location-dependent. For example, the 108 kHz signal only appears at sites 041 through 050. The 80, 90, 100, and 108 kHz signals are missing from sites 104-051 through 104-056. The 100 kHz signal does not appear at many blocks of sites. The 80 and 90 kHz signal does not appear at sites 106-001 through 106-005.

   These site-dependent factors suggest that a different set of sites probably would yield different signal levels.

2. Low levels of Loran-C signal indicated by the symbol < and implied by some cases where the symbol - was used, are not included in the mean and standard deviations. Thus, the mean levels of Loran-C signals are artificially high and the standard deviations are artificially low.

3. The impulsive noise levels are extremely dependent upon locations. Sometimes the peak amplitude of impulsive noise varied more than 50 dB over distances as short as 100 feet. Thus the levels shown represent only that at the precise measurement location.

4. The CW signal at 119 kHz appeared in all 3-axis views except at site 106-005. The source of the 119 kHz signal is believed to be a USN transmitter in central California. The mean value of this signal is probably reasonable.

TABLE 6-1. SIGNAL AND NOISE LEVELS

SITE NO.	LORAN-C SIGNALS				NOISE	CW SIGNALS				
	M	W	X	Y	N	80	90	100	108	119
106-001	-86	-88	-86	-76	0	0	0	-98	0	-100
106-002	-83	-83	-79	-76	0	0	0	-98	0	-96
106-003	-81	-85	-81	-78	-71	0	0	-86	0	-98
106-004	-76	-78	-76	-73	-84	0	0	-92	0	-99
106-005	-91	-88	-80	-76	0	0	0	0	0	0
106-006	<	-90	-83	-75	0	-96	0	0	-94	-96
106-007	-83	-81	-73	-66	0	-85	0	0	-86	-84
106-008	-76	-73	-68	-61	0	-83	0	0	-77	-81
106-009	<	-71	-69	-66	0	0	-87	-86	0	-87
106-010	<	-75	-73	-66	-83	-85	0	0	-76	-75
109-011	<	-83	-79	-70	0	-95	-95	0	0	-87
109-012	-80	-75	-68	-63	0	-90	-88	0	0	-84
109-013	-85	-83	-73	-63	0	-95	-93	0	0	-85
109-014	-78	<	-73	-63	0	0	0	0	0	-85
109-015	-78	<	-73	-63	0	-96	-93	-87	0	-87
109-016	-73	-74	-69	-64	0	-94	-95	-90	0	-86
109-017	--	--	--	-70	0	0	0	-71	0	-92
109-018	-85	-83	-73	-63	0	0	0	0	0	-86
109-019	-70	-70	-65	-63	0	-95	-95	0	0	-91
109-020	-78	-76	-66	-66	0	-95	-96	0	0	-95
108-021	-77	-77	-68	-67	0	-96	-96	0	0	-96
108-022	-76	-75	-68	-66	0	-95	-93	0	0	-90
108-023	-74	-72	-66	-62	0	-94	-85	0	-92	-83
108-024	--	--	--	-78	0	-87	-87	-86	0	-87
108-025	--	--	--	--	-90	0	0	-67	0	-85
108-026	-75	-75	-65	-65	0	0	-95	0	0	-90
108-027	-72	-73	-69	-64	0	-95	-94	0	0	-87
108-028	-76	-78	-73	-65	0	-94	-90	0	0	-91
108-029	<	<	-78	-73	0	0	0	-87	0	-95
108-030	-77	-78	-70	-66	0	-92	-90	0	0	-87

TABLE 6-1. SIGNAL AND NOISE LEVELS (CONTINUED)

SITE NO.	LORAN-C SIGNALS				NOISE	CW SIGNALS				
	M	W	X	Y	N	80	90	100	108	119
107-031	--	--	-72	-63	-75	-86	-89	0	0	-87
107-032	-83	-83	-71	-67	0	-96	-93	0	0	-88
107-033	-77	-78	-78	-66	-78	0	0	0	0	-92
107-034	--	-74	-71	-66	0	-87	-93	0	0	-92
107-035				NO	MEASUREMENT					
107-036	--	--	-79	-80	-88	0	0	0	0	-93
107-037	-71	-73	-65	-63	0	0	-85	0	0	-86
107-038	-73	-73	-63	-63	0	0	-85	0	0	-86
107-039	-73	-73	-66	-63	0	0	-85	0	0	-89
107-040	-75	-73	-66	-63	0	-90	-81	0	0	-87
110-041	-78	-83	-71	-66	0	-86	-86	0	-78	-86
110-042	-76	<	-75	-69	0	-81	-84	0	-84	-87
110-043				NO	MEASUREMENT					
110-044	-85	<	-75	-75	0	-90	0	0	-85	-92
110-045	-94	-95	-74	-70	0	-92	-85	0	-79	-94
110-046	--	--	--	--	--	-75	-70	-79	-66	-70
110-047	--	--	--	--	0	-77	-72	-85	-70	-79
110-048	-67	-69	-66	-66	0	-76	-78	0	-67	-85
110-049	-70	-94	-64	-64	0	-85	-77	0	-79	-85
110-050	-76	-76	-78	-78	0	-90	-87	0	-94	-85
104-051	<	<	-70	-68	-75	0	0	0	0	-90
104-052	-85	-85	-73	-73	0	0	0	0	0	-95
104-053	-74	-74	-66	-62	0	0	0	0	0	-87
104-054	-78	-78	-66	-64	0	0	0	0	0	-90
104-055	-80	-80	-70	-68	-80	0	-95	0	0	-95
104-056	-78	-78	-72	-72	0	0	0	0	0	-95
N	35.0	35.0	43.0	45.0	9.0	30.0	32.0	9.0	14.0	47.0
$\overline{x}$	-77.31	-77.46	-70.47	-66.71	-80.44	-89.23	-88.03	-82.00	-80.50	-87.57
σ	5.36	5.93	4.37	4.57	6.27	6.29	6.86	7.98	9.22	5.06

The data in Table 6-1 can be used to compare measured noise and RFI with receiver performance. Such a comparison must take into consideration the complex combination of impulsive noise intervals and amplitudes, the non-flat properties of the noise impulses, the CW signals at various frequencies and various levels, the amplitudes of the Loran-C signals, and the signal processing techniques employed by each model of Loran-C receiver tested.

The non-flat properties of impulsive noise across the relatively narrow band of frequencies generally considered necessary for successful Loran-C receiver performance are of special interest (assumed to be about 20 kHz wide centered at 100 kHz). Usually noise is assumed to be flat across the receiver bandwidth; however, most measured examples of impulsive noise were non-flat as shown in the 3-axis views for sites 108-025, 107-031, 107-033, 107-034, 107-036, 110-047, 104-051, and 104-055 in Appendix A.

Intermittent impulsive noise conditions were observed at sites 107-034 and 110-046.

Table 6-2 provides an overall summary of noise and CW signals at each site and allows the reader to compare general noise and CW signal conditions to site descriptors. The site identification numbers employed in Tables 5-2 and 6-1 are used as well as the site descriptors contained in Table 5-2. A T was added to the power line status whenever a nearby utility high voltage transmission line was noted. The remaining columns are as follows:

Column Heading

Noise	0 indicates no noise. 1 indicates the presence of impulsive noise in the 100 $\pm$ 10 kHz band.
CW = 80 CW = 90 CW = 100 CW = 108 CW = 118	0 indicates no CW signals. 1 indicates a weak CW signal (< 10 dB above receiver noise). 2 indicates a strong CW signal ($\geq$ 10 dB above receiver noise).

TABLE 6-2. COMPARISON OF SITE PARAMETERS WITH MEASURED RESULTS

SITE PARAMETERS			MEASURED RESULTS					
SITE NO.	SITE CAT.*	POWER LINE CAT.†	NOISE	CW = 80	CW = 90	CW = 100	CW = 108	CW = 119
106-001	C	1	0	0	0	1	0	1
106-002	R	0 T	0	0	0	1	0	1
106-003	C	1 T	1	0	0	2	0	1
106-004	I	2	1	0	0	1	0	1
106-005	R	0	0	0	0	0	0	0
106-006	R	0 T	0	1	0	0	1	1
106-007	C	1	0	2	0	0	2	2
106-008	O	0	0	2	0	0	2	2
106-009	I	1	0	0	1	2	0	2
106-010	I	2 T	1	2	0	0	2	2
109-011	R	0	0	1	1	0	0	2
109-012	O	0	0	1	2	0	0	2
109-013	C	0	0	1	1	0	0	2
109-014	C	1	0	0	0	0	0	2
109-015	C	1	0	1	1	2	0	2
109-016	I	1 T	0	1	1	1	0	2
109-017	I	2 T	0	0	0	2	0	1
109-018	I	0	0	0	0	0	0	2
109-019	R	0	0	1	1	0	0	1
109-020	R	0	0	1	1	0	0	1

* Site category: C - commercial, R - residential, I - industrial, O - open.

† Power lines show number of lines present (one side or both sides of street): 1 - one side, 2 - both sides, underline of number - van directly under lines, T - nearby utility transmission line.

TABLE 6-2. COMPARISON OF SITE PARAMETERS WITH MEASURED RESULTS (CONTINUED)

SITE PARAMETERS			MEASURED RESULTS					
SITE NO.	SITE CAT.*	POWER LINE CAT.†	NOISE	CW = 80	CW = 90	CW = 100	CW = 108	CW = 119
108-021	I	1 T	0	1	1	0	0	1
108-022	I	0	0	1	1	0	0	1
108-023	O	0	0	1	2	0	1	2
108-024	I	$\underline{1}$	1	2	2	2	0	2
108-025	R	1	1	0	0	2	0	2
108-026	R	0	0	0	1	0	0	1
108-027	R	1	0	1	1	0	0	2
108-028	C	0	0	1	1	0	0	1
108-029	C	$\underline{1}$	0	0	0	2	0	1
108-030	C	1	0	1	1	0	0	2
107-031	I	1	1	2	2	0	0	2
107-032	C	1	0	1	1	0	0	2
107-033	I	1	1	0	0	0	0	1
107-034	I	$\underline{2}$	0	1	1	0	0	1
107-035	C	0	-	-	-	-	-	-
107-036	C	0	1	0	0	0	0	1
107-037	R	0	0	0	1	0	0	2
107-038	R	0	0	0	1	0	0	2
107-039	R	0 T	0	0	1	0	0	2
107-040	O	0 T	0	1	1	0	0	2

* Site category: C - commercial, R - residential, I - industrial, O - open.

† Power lines show number of lines present (one side or both sides of street): 1 - one side, 2 - both sides, underline of number - van directly under lines, T - nearby utility transmission line.

TABLE 6-2. COMPARISON OF SITE PARAMETERS WITH MEASURED RESULTS (CONTINUED)

SITE PARAMETERS			MEASURED RESULTS					
SITE NO.	SITE CAT.*	POWER LINE CAT.†	NOISE	CW = 80	CW = 90	CW = 100	CW = 108	CW = 119
110-041	R	0	0	2	1	0	2	2
110-042	C	1 (underlined)	0	2	1	0	2	2
110-043	O	0	-	-	-	-	-	-
110-044	R	1	0	1	0	0	2	1
110-045	C	1	0	1	2	0	2	1
110-046	I	1 (underlined) T	1	2	2	2	2	2
110-047	C	2 (underlined) T	1	2	2	1	2	2
110-048	I	1 T	0	2	2	0	2	2
110-049	I	0	0	2	2	0	2	2
110-050	R	1	0	1	2	0	1	2
104-051	R	1	1	0	0	0	0	1
104-052	C	1 T	0	0	0	0	0	1
104-053	O	0	0	0	0	0	0	2
104-054	R	1	0	0	0	0	0	1
104-055	R	0	1	0	1	0	0	1
104-056	C	1 (underlined)	0	0	0	0	0	1
CW or Noise 0			42	23	22	41	40	1
CW or Noise 2			12	20	22	5	3	23
CW 2			0	11	10	8	11	30

* Site category: C - commercial, R - residential, I - industrial, O - open.

† Power lines show number of lines present (one side or both sides of street): 1 - one side, 2 - both sides, underline of number - van directly under lines, T - nearby utility transmission line.

Impulsive noise was observed in the standard 3-axis views or in the additional 3-axis views at 12 out of the 54 sites. Ten of these 12 sites had nearby utility distribution lines as shown in the Gould site survey. The two sites that had impulsive noise conditions, but did not have a distribution line indicated in the Gould site categorization (sites 107-036 and 104-055) were close to a nearby distribution line that did not fit the Gould categorization. Thus, whenever impulsive noise was observed, a utility distribution line was nearby.

Seven distribution lines directly overhead the measurement vehicles did not emanate impulsive or other noise at levels sufficient to exceed the 3-axis threshold level setting ($\approx$ -100 dBm). In addition, fourteen distribution lines located across the street from the measurement vans did not emanate sufficient impulsive or other noise to exceed the threshold level of the 3-axis views.

CW signals were observed at many of the Phase II sites. A total of 13 of the 54 sites had CW signals at or very close to 100 kHz. The signal strength was less than 10 dB above the measurement system receiver noise level at five sites and equal to or greater than 10 dB above the receiver noise at eight sites.

At 90 kHz CW signals were observed at 32 of the 54 sites. Twenty-two of these cases resulted in signals less than 10 dB above the receiver noise, and ten cases gave signals equal to or exceeding 10 dB above the receiver noise.

At 80 kHz CW signals were found at 31 of the 54 sites. Twenty of these cases resulted in signals less than 10 dB above receiver noise, and eleven cases gave signal levels equal to or greater than 10 dB above receiver noise.

At 108 kHz CW signals were found at 14 of the 54 sites. Three of these cases resulted in signals less than 10 dB above the receiver noise level, and eleven gave signal levels equal to or greater than 10 dB above receiver noise.

The 119 kHz CW communications signal appeared at 53 of the 54 sites. Twenty-three cases gave signal levels less than 10 dB above receiver noise, while 30 cases gave signal levels equal to or greater than 10 dB above receiver noise.

A Loran-C receiver experienced CW RFI at 100 kHz at five sites and excessive CW RFI at eight sites. The impact of the CW signals at 80, 90, 108, and 118 kHz on Loran-C performance would depend upon the RF filter employed in the receiver and upon signal detection processes employed by each individual receiver. The significance of the CW signals at or beyond Loran-C band limits must be examined for each individual receiver.

While the sources of the CW signals were not specifically identified (except for traffic control and telephone line CW signals), the 80, 90, 100, and 108 kHz signals appeared at distinct sequences of sites. Also, strong CW signals tended to cluster at sequences of sites. These patterns are typical of near-field reception of power line carrier signals. Also, the 100 kHz CW signal was associated with the power carrier signal at 100 kHz which was identified in Sections 3 and 4.

6.3 SUPPLEMENTARY MEASUREMENTS

The supplementary measurements described in Section 3.3 must be considered when evaluating results of the fixed site measurements. The supplementary measurements show very strong spatial variations in both noise and CW signals as the measurement van moved over very short distances. Furthermore, the supplementary measurements show that all cases of impulsive noise and most CW signals emanate from nearby metallic devices (power lines, traffic control devices, telephone lines, etc.). Near-field radiation characteristics are evident from the data and from the observed physical relationships involved. The actual impulsive noise sources themselves may have been blocks or miles from the measurement site, but the radiation mechanism and coupling into the Loran-C whip antenna was primarily a near-field process.

6.4 NOISE AND CW SIGNAL MAPPING

Previous measurements of urban and suburban area radio noise suggested that impulsive noise and CW signals might be combined by some convenient method which could be used to generate noise/RFI contour maps for the portions of Los Angeles examined in the Phase I and Phase II measurements. However, the near-field properties of the noise and most CW signals resulted in small isolated areas of noise/RFI where large changes in level occurred over distances as small as 10 feet to 30 feet. These active areas were separated by low noise areas where conventional atmospheric noise levels were observed. Thus, any realistic noise mapping program would require the very fine scale mapping of a very large area where significant contours would often be spaced about 10 feet to 20 feet apart. The measurement task to support the mapping of noise and RFI for Los Angeles would be formidible. Obviously, the conventional contour mapping of noise and RFI is not recommended.

A more productive approach would be to better understand the near-field radiation models of each significant source and then ascertain the noise or CW activity associated with each possible source. Such data could be used as the basis for regionally-oriented fine scale contour maps.

Each relatively small area of high noise was usually associated with a single radiator of noise. Also, each area of high CW signal level (except for the 119 kHz communications signal) appeared to be associated with a single radiator or a very few radiators. Noise or CW signals from multiple sources were only rarely identified. Thus, the conventional techniques of composite mapping of various kinds of noise from multiple sources could not be used to describe the noise and RFI environment encountered by vehicular Loran-C receivers operated in Los Angeles.

Noise and CW signals were generally lower in level in the main downtown area of Los Angeles than in the urban and suburban areas surrounding downtown. The low levels of downtown noise and CW signals were associated with the lack of overhead utility distribution lines (most downtown power distribution was underground), the absence of utility transmission lines, and the attenuation of all signals near 100 kHz when near multistory structures.

Sufficient measurements were taken at and around site 109-018 (Watson Center/Wilmington) to establish approximate fine scale contours of peak impulsive noise levels for the immediate area. Figure 28 shows the main physical features of the site including the location of a nearby utility distribution line which radiated significant impulsive noise. The distribution line ended about 100 feet from the 109-018 site. Ten dB contours of noise (see Figures 5-13, 5-14, 5-15, and A-29 for noise detail) are superimposed on the physical map. The contours of peak impulsive noise level show very low noise levels at site 109-018 itself and high noise levels when closer to the distribution line. The noise level decreased somewhat with distance along the distribution line along Watson Center, causing the contours to pinch inward near the top of the area shown. The distance scale on the map shows the relatively small area with significant levels of impulsive noise. A vehicle with a Loran-C receiver turning off Wilmington onto Watson Center would abruptly encounter impulsive noise shortly after the turn. The noise would gradually decrease in level as the vehicle proceeded along Watson Center.

The noise contours in Figure 6-1 show the relationship between the impulsive noise encountered by a Loran-C receiver installed in a vehicle and the noise radiator (a 13.6 KV distribution line). Similar contour maps can be established for all other noise and CW signals found in the Phase I and Phase II effort with a few additional measurements and a description of the physical properties of the noise radiator.

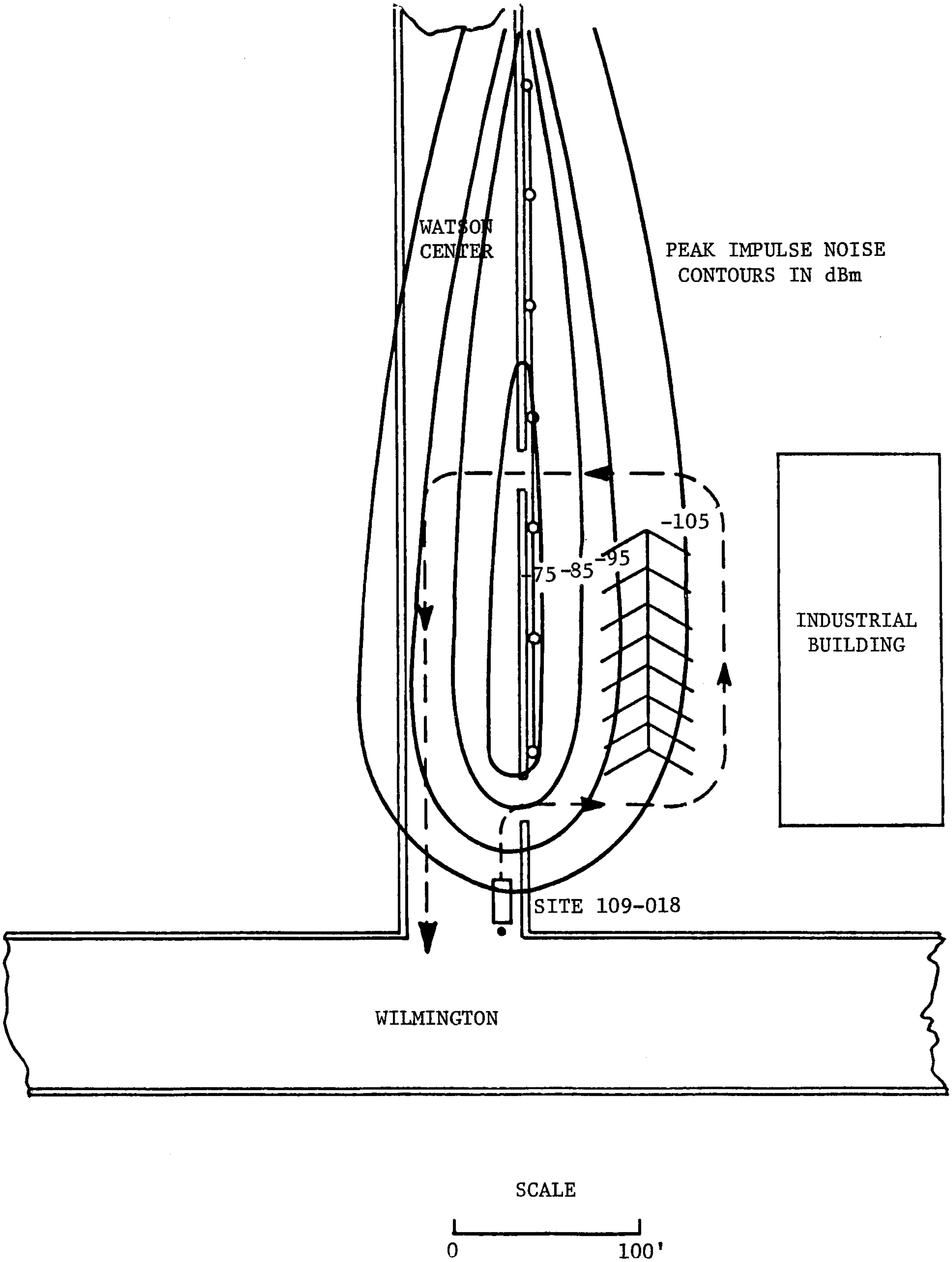

FIGURE 6-1. PHYSICAL LAYOUT OF SITE 109-018

6.5 NOISE DESCRIPTORS AND OTHER MEASUREMENTS

A number of descriptors of radio noise have appeared in the literature including peak, quasi-peak, rms, and average values, as well as various distributions of amplitudes, zero crossing rates, intervals, and widths. Hagn has reviewed and summarized the various definitions and fundamental parameters of noise and RFI (4). The government has recommended that noise power be used as the basic noise parameter (5); however, other additional measurements of noise are acknowledged as necessary for specific analysis tasks. The most widely used reference for received noise levels is the CCIR Report 322 (6), which is based upon noise power. Spaulding and his associates have published convenient noise definitions which are consistent with CCIR and government recommendations (7-9), and they have presented a number of excellent measurements of noise affecting various communications systems. A recent book by Skomal (10) summarizes much of the available information and data on man-made noise. Feldman has presented data on radio noise levels in a study specifically directed toward the rural area noise environment encountered by low frequency navigation systems such as Loran-C (11).

Most of the above referenced descriptors and definitions of radio noise can be related to the 3-axis views presented in this report, and the basic information to obtain noise values in accordance with the various descriptors is contained in the digital data stream which forms the views. These digital data are available at the digital interface on the EMTEL display. Also, the 3-axis views can be hand-scaled to derive sufficient information for approximate values of peak noise, noise power, interval times, and other factors.

The author prefers to relate the 3-axis views to the terminology and definitions used by Spaulding (9) and many others, where mean noise power is:

$$p_n = f_a(k\,T_o\,b)$$

where p_n = mean noise power in watts

f_a = effective antenna noise factor

k = Boltzman's constant τ $1.38 \cdot 10^{-23}$ Joules/°K

T_o = reference temperature (288°K)

b = receiver noise power bandwidth in Hz

T_a = effective antenna temperature in the presence of external noise.

The above expression for p_n can be reduced to:

$$P_n = F_a + B - 204 \quad \text{dBw}$$

which is the power available from the terminals of an equivalent lossless antenna where

P_n = available noise power in dBw

F_a = 10 log f_a, the effective antenna noise figure

B = 10 log b.

The corresponding rms field strength measured by the 108 inch whip antenna (length << λ) is given by:

$$E_n = F_a + 20 \log f + B - 95.5 \quad \text{dB}(1\mu\text{V/m})$$

where E_n = rms field strength for the bandwidth b

f = frequency in MHz

B = 10 log b.

The amplitude scales for the 3-axis views in this report can be recalibrated in terms of either P_n or E_n from the above relationships and from data contained the the two-line code on each 3-axis view.

The dB difference between average noise voltage and rms noise voltage, called V_d, is a convenient indicator of the degree of impulsiveness where:

$$V_d = -20 \log \frac{V_{av}}{V_{rms}} .$$

An excellent indicator of the amplitude properties of a given sample of noise is the amplitude probability distribution (APD), which is the fraction of total time, T, for which the noise envelope is above level V_i.

$$APD = \text{Prob}[V \geq V_i] = 1 - P(V).$$

The 3-axis views shown in this report also permit the viewer to very rapidly scale impulse intervals due to the unique time synchronization of most impulses to the power line frequency. Distributions of pulse spacing intervals can be simply established for most cases in that only a few sub-multiples of 16.6 ms are involved in the impulse spacings.

Data on the mean power level of noise at and near 100 kHz are given by CCIR (6) and Feldman (11). These sources and all other available published sources indicate that atmospheric radio noise should be the predominant noise limiting the performance of Loran-C receivers. However, the measurements described in this report showed that man-made radio noise was the predominant noise limiting the performance of Loran-C receivers installed in vehicles and operated in the Los Angeles area. The sources of data for CCIR Report 322 and Feldman were from isolated and remote radio noise measurement sites which did not include the near-field coupling to noise and CW sources found to be of major concern in the Los Angeles area. Loran-C systems designed for use in city areas must take into account the properties of the noise environment of the urban and suburban area.

7. CONCLUSIONS

The measurements of man-made noise and RFI in the urban and suburban areas of Los Angeles provided data useful in assessing the performance of Loran-C receivers operated in and around the region. Vehicular Loran-C receivers moving along the streets and highways of Los Angeles would be subjected to a wide variety of radio environments. At times low natural noise levels would result in excellent Loran-C receiver performance. The extremely rapid transition from low level natural noise conditions to very high levels of impulsive noise, or very high levels of CW RFI, or combinations of the two states, must be carefully considered by the designers of vehiclular Loran-C receivers.

Early in the measuerment program the possibility of the construction of noise maps showing portions of Los Angeles containing high noise levels was discussed among the measurement participants. The data show that any effective contour mapping of noise levels must be based upon contour intervals of a few tens of feet rather than the larger intervals implied by other available noise maps. Obviously, a realistic contour map of noise cannot be generated for the Los Angeles area with conventional radio noise measurement and mapping techniques.

The very rapid amplitude change with distance for radio noise associated with utility power lines suggests that cities confining most overhead distribution lines to alleys in mid-block would have lower street noise levels than cities with overhead distribution lines running along street edges. Underground power lines would also result in low street radio noise levels. Of special interest was the general observation that radio noise levels in the downtown area of Los Angeles (where power lines were largely underground) were generally much lower than in the area surrounding downtown. This null in noise level in the center of the large urban area of Los Angeles was not consistent with the generalized urban area noise model of Skomal (12 which gave a maximum for noise levels in the center of the urban area. Skomal's model also suggests that urban and suburban area radio noise can be adequately described with conventional contour maps. This is not consistent with the "hot-spot" areas of man-made noise found in Los Angeles.

The inductive or near-field coupling between most noise and RFI radiators and a vehicular Loran-C antenna was obvious, once encountered. This aspect of a noise source-to-sink model has not been emphasized in the recent literature on man-made radio noise, but it was of primary importance in understanding the noise environment encountered by vehicular Loran-C receivers.

The various primary sources of RFI (traffic control sensors, unshielded overhead telephone lines, and power line carrier communications) also coupled into the vehicular Loran-C antenna with inductive or near-field modes. Very low power and physically small sources produced very large input signals into the antenna whenever the measurement van was physically close to a source.

A single noise or RFI source was often the major contributor to the undesired radio environment. At most only a few sources were involved at any specific measurement location. Complex mixtures of noise and RFI from a large number of sources were not found. This suggests that a program to rapidly locate and identify each primary source of noise and RFI would be technically feasible. However, the next obvious step, noise and RFI suppression at each source would involve complex issues of radio spectrum management, adequacy of incidental radiation rules, inductive or near-field radiation considerations in noise and RFI models, cost of control measures versus cost of benefits, and other related factors.

APPENDIX A

3-AXIS VIEWS FOR FIXED SITES

LIST OF 3-AXIS VIEWS

Page

1/22/79, 0831, 106-001 132
1/22/79, 0845, 106-002 133
1/22/79, 0905, 106-003 (under 12 KV line) 134
1/22/79, 0928, 106-003 (under 12 KV line) 135
1/22/79, 0946, 106-004 136
1/22/79, 0948, 106-004 137
1/22/78, 1017, 106-005 138
1/22/79, 1334, 106-006 139
1/22/79, 1036, 106-006 140
1/22/79, 1131, 106-007 141
1/22/79, 1142, 106-008 142
1/22/79, 1159, 106-009 143
1/22/79, 1222, 106-010 144
1/22/79, 1251, 109-011 145
1/22/79, 1304, 109-012 146
1/22/79, 1307, 109-012 147
1/22/79, 1320, 109-013 148
1/22/79, 1327, 109-013 149
1/22/79, 1332, 109-013 150
1/23/79, 0756, 109-014 151
1/23/79, 0808, 109-015 152
1/23/79, 0822, 109-015 153
1/23/79, 0831, 109-016 154
1/23/79, 0844, 109-017 155
1/23/79, 0933, 109-018 156
1/23/79, 0947, 109-019 157
1/23/79, 1005, 109-020 158
1/23/79, 1017, 108-021 159
1/23/79, 1026, 108-022 160
1/23/79, 1138, 108-023 161
1/23/79, 1146, 108-024 162

LIST OF 3-AXIS VIEWS (Continued)

Page

1/23/79, 1203, 108-025 163
1/23/79, 1218, 108-025 164
1/23/79, 1221, 108-025 165
1/23/79, 1242, 108-026 166
1/23/79, 1252, 108-027 167
1/23/79, 1323, 108-028 168
1/23/79, 1308, 108-029 169
1/23/79, 1333, 108-030 170
1/24/79, 0814, 107-031 171
1/24/79, 0816, 107-031 172
1/24/79, 0819, 107-031 173
1/24/79, 0833, 107-032 174
1/24/79, 0834, 107-033, Location 1 175
1/24/79, 0838, 107-033, Location 1 176
1/24/79, 0901, 107-033, Location 2 177
1/24/79, 0902, 107-033, Location 2 178
1/24/79, 0905, 107-034 179
1/24/79, 0916, 107-034 180
1/24/79, 0923, 107-034 181
1/24/79, 1001, 107-036 182
1/24/79, 1006, 107-037 183
1/24/79, 1011, 107-038 184
1/24/79, 1035, 107-039 185
1/24/79, 1040, 107-040 186
1/25/79, 0752, 110-041 187
1/25/79, 0757, 110-041 188
1/25/79, 0803, 110-042 189
1/25/79, 0810, 110-042 190
1/25/79, 0817, 110-044 191
1/25/79, 0823, 110-044 192
1/25/79, 0833, 110-045 193

LIST OF 3-AXIS VIEWS (Continued)

Page

1/25/79, 0846, 110-046 194
1/25/79, 0853, 110-046 195
1/25/79, 0851, 110-046 196
1/25/79, 0904, 110-047 197
1/25/79, 0914, 110-047 198
1/25/79, 0932, 110-048 199
1/25/79, 0948, 110-049 200
1/25/79, 0958, 110-050 201
1/25/79, 1228, 104-051 202
1/25/79, 1227, 104-051 203
1/25/79, 1230, 104-051 204
1/25/79, 1238, 104-052 205
1/25/79, 1253, 104-053 206
1/25/79, 1306, 104-054 207
1/25/79, 1322, 104-055 208
1/25/79, 1321, 104-055 209
1/25/79, 1325, 104-055 210
1/25/79, 1332, 104-056 . . . . 211/212

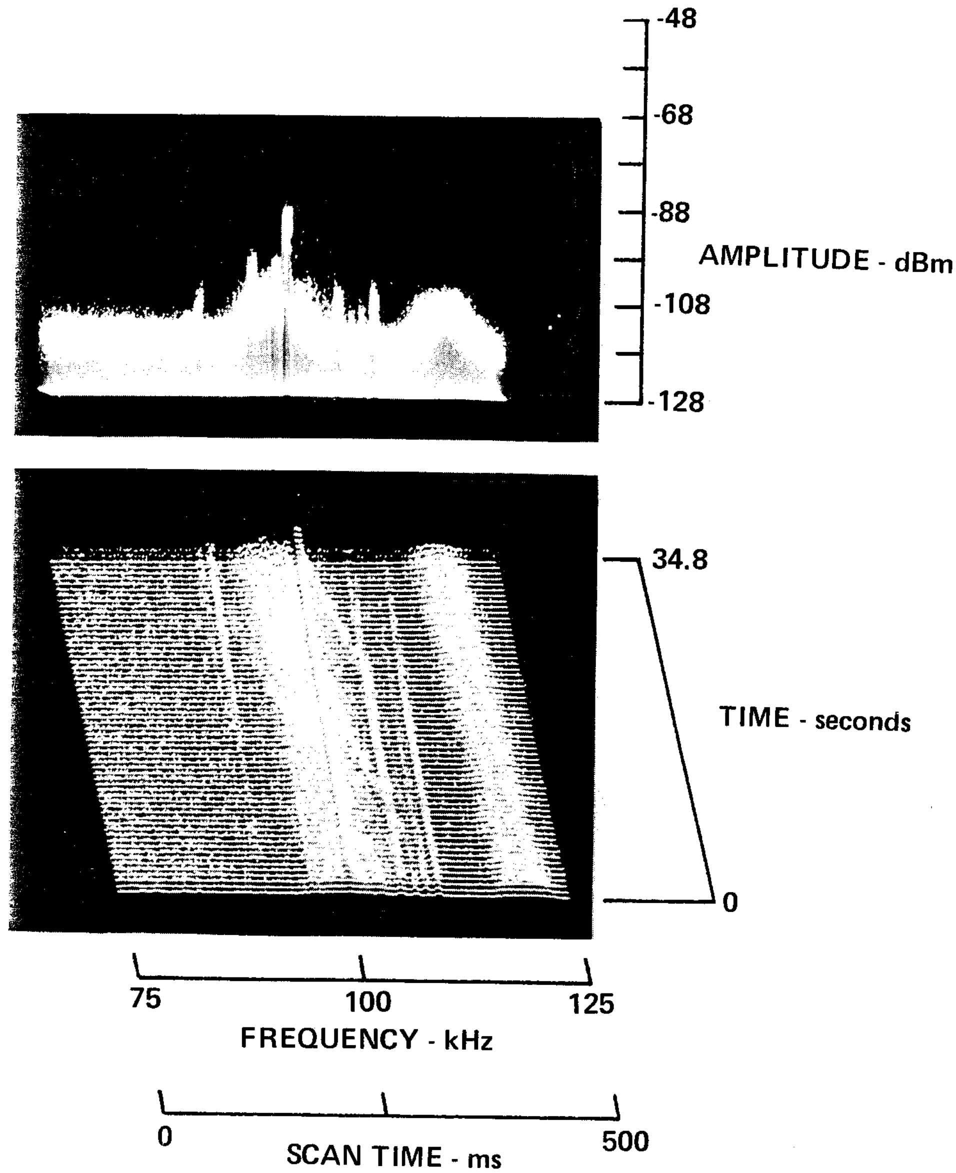

1-22-79, 0831, 106-001
HP140, Whip, F100, W50, IF3, ST 500, A -30/0/+18/BPF

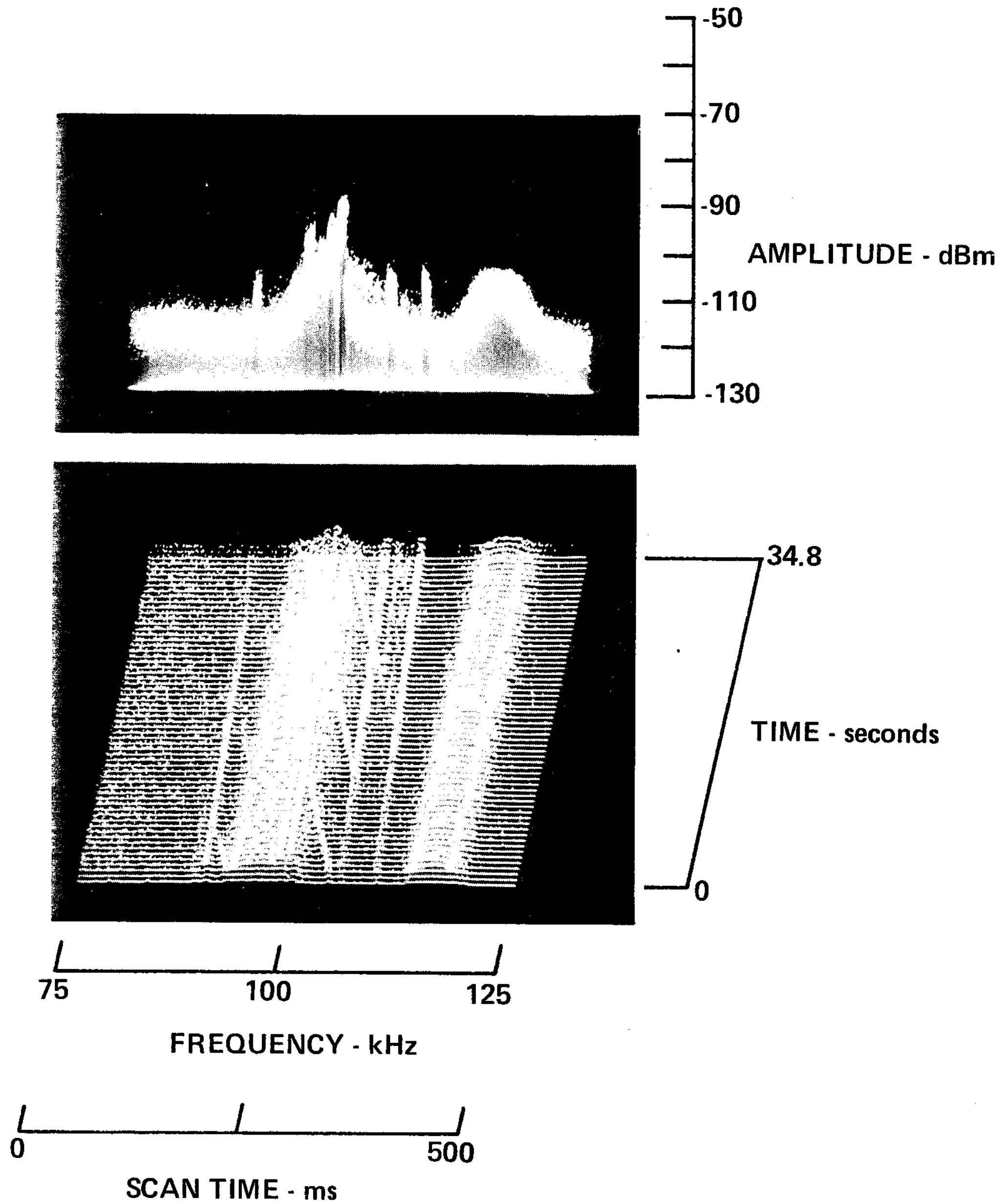

1-22-79, 0845, 106-002
HP140, Whip, F100, W50, IF3, ST 500,A -32/0/+18/BPF

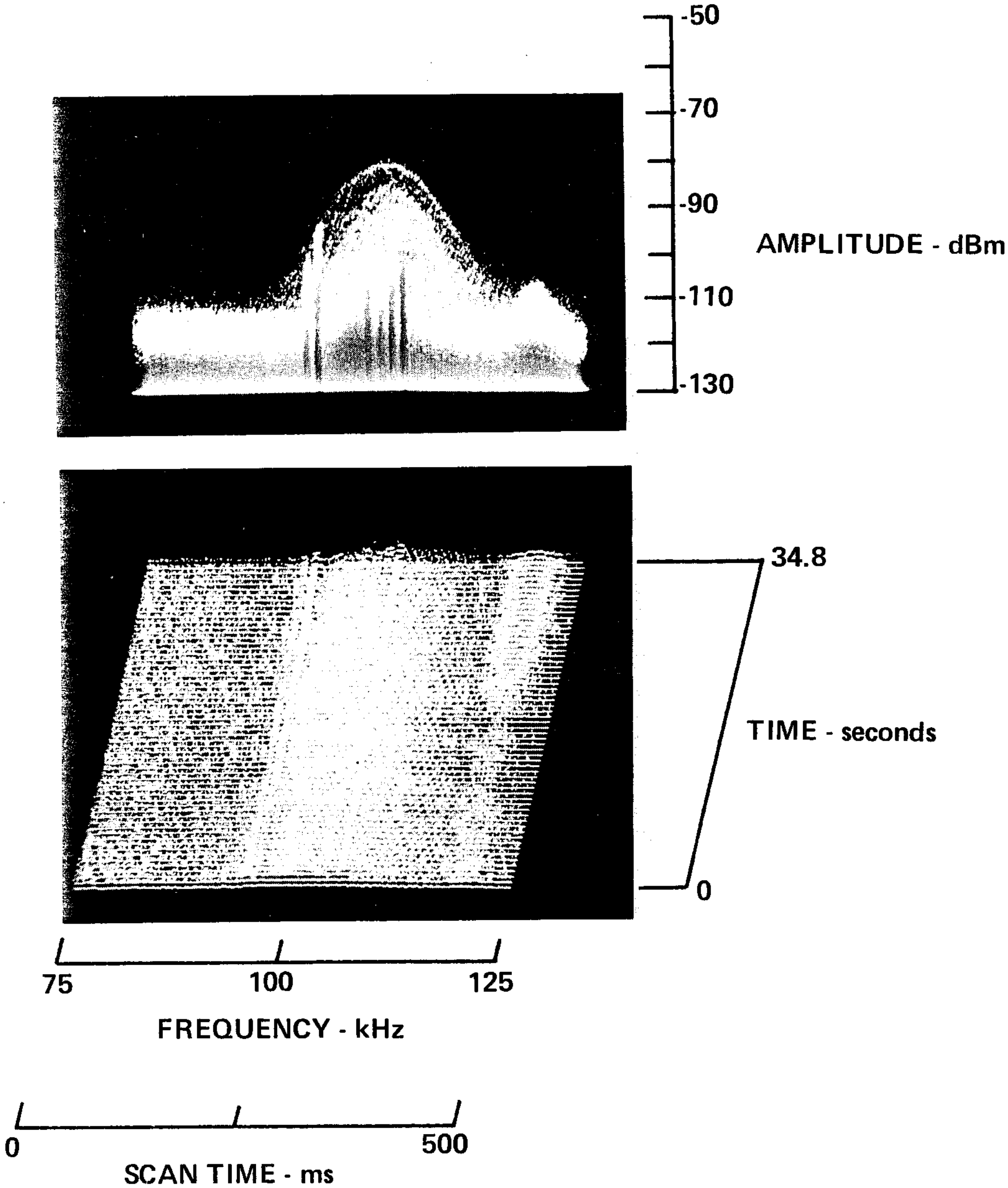

1-22-79, 0905, 106-003 (under 12 kV line)
HP140, Whip, F100, W50, IF3, ST 500, A -32/0/+18/BPF

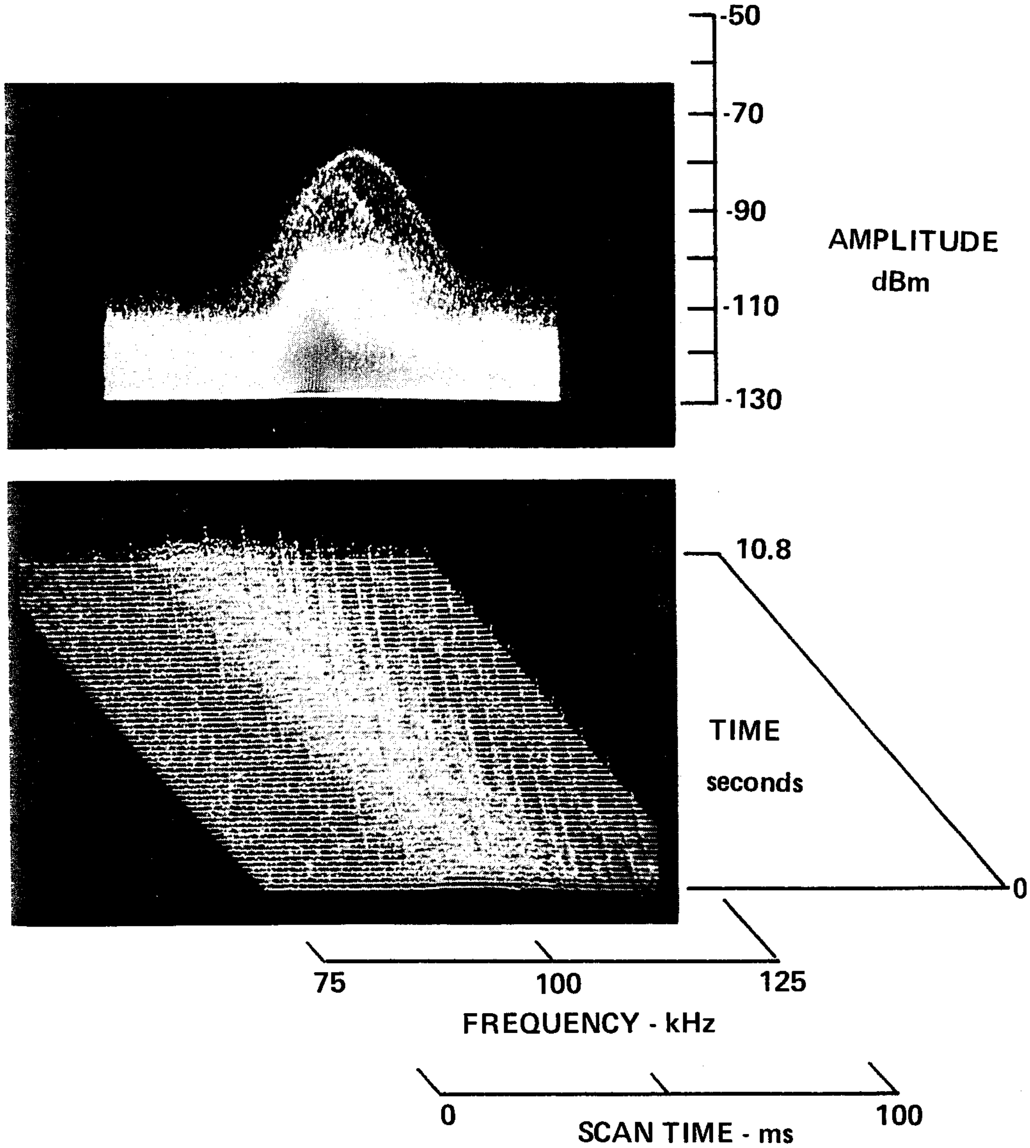

1-22-79, 0928, 106-003 (under 12 kV line)
HP140, Whip, F100, W50, IF3, ST 100, A -32/0/+18/BPF

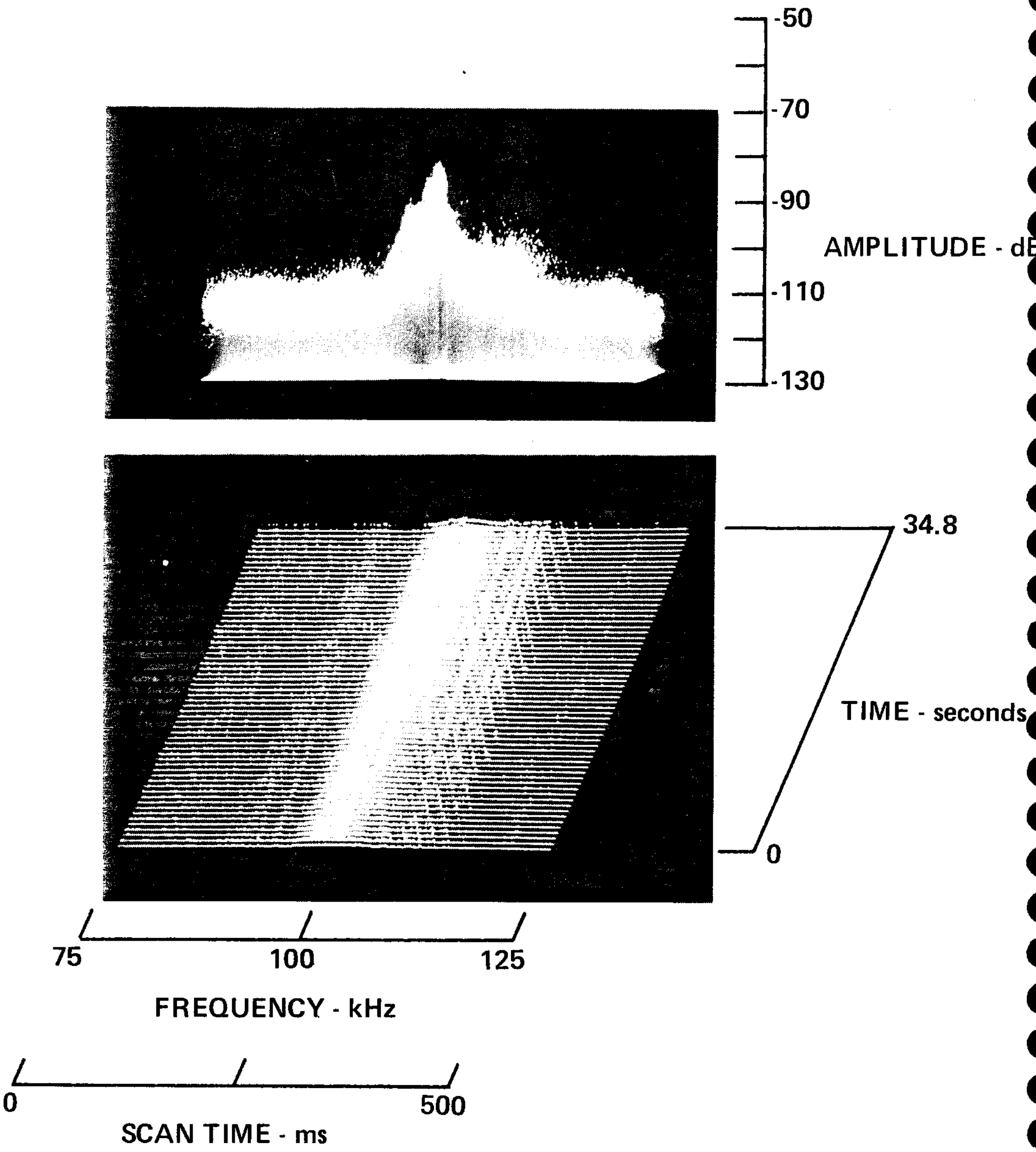

1-22-79, 0946, 106-004
HP140, Whip, F100, W50, IF3, ST 500, A -32/0/+18/BPF

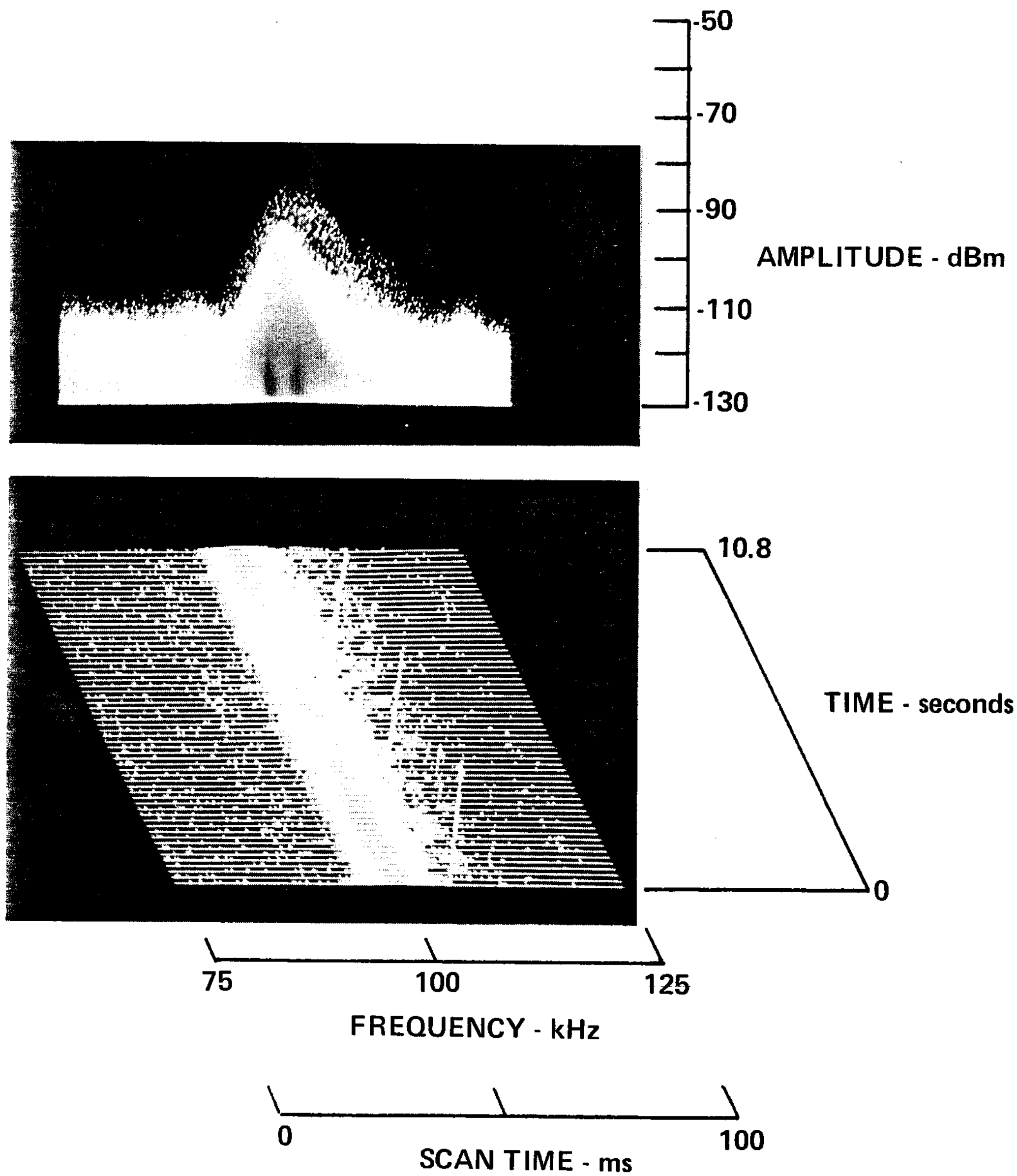
-50
-70
-90
AMPLITUDE - dBm
-110
-130
10.8
TIME - seconds
0
75
100
125
FREQUENCY - kHz
0
100
SCAN TIME - ms

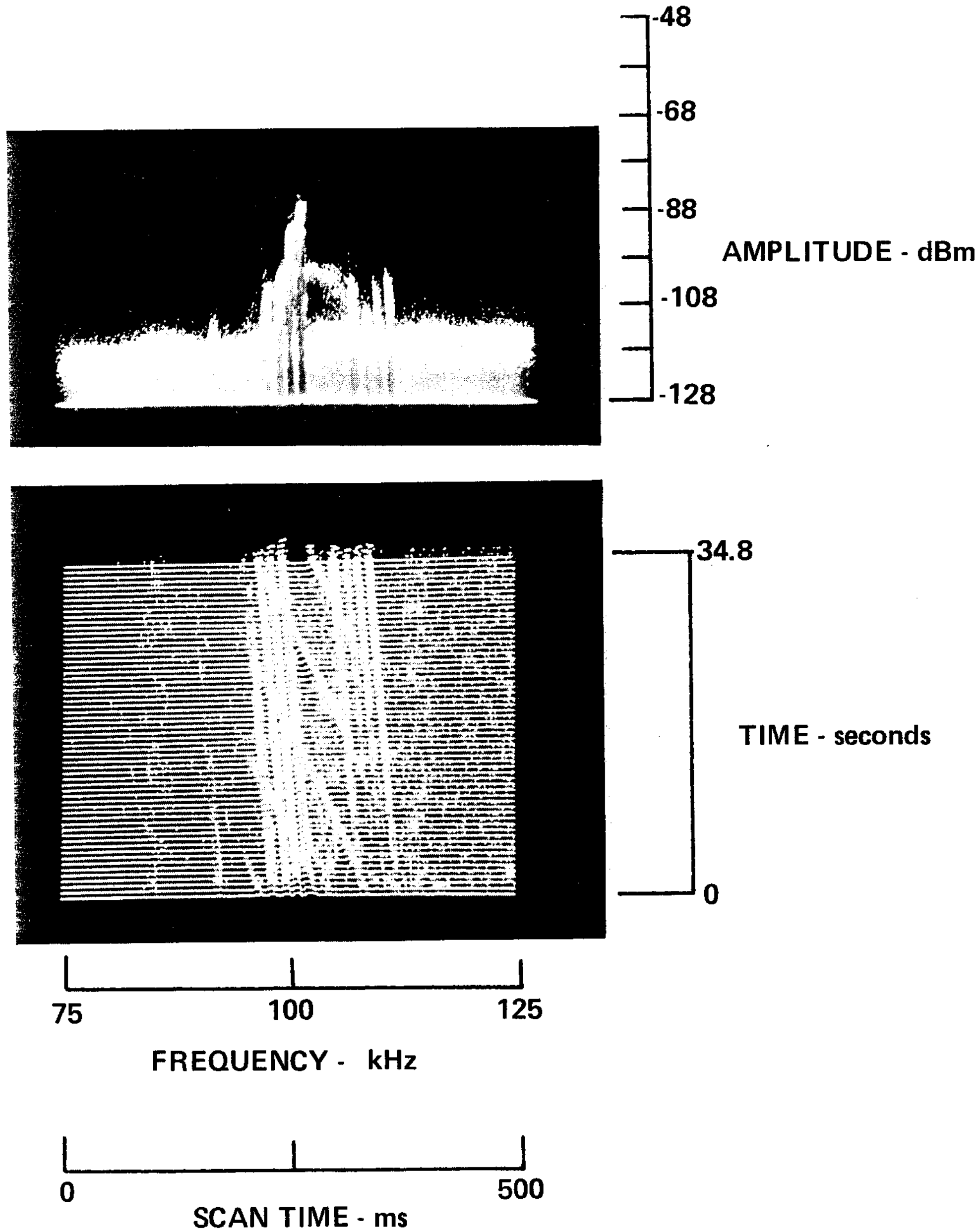

1-22-78, 1017, 106-005
HP140, Whip, F100, W50, IF3, ST 500, A -30/0/+18/BPF

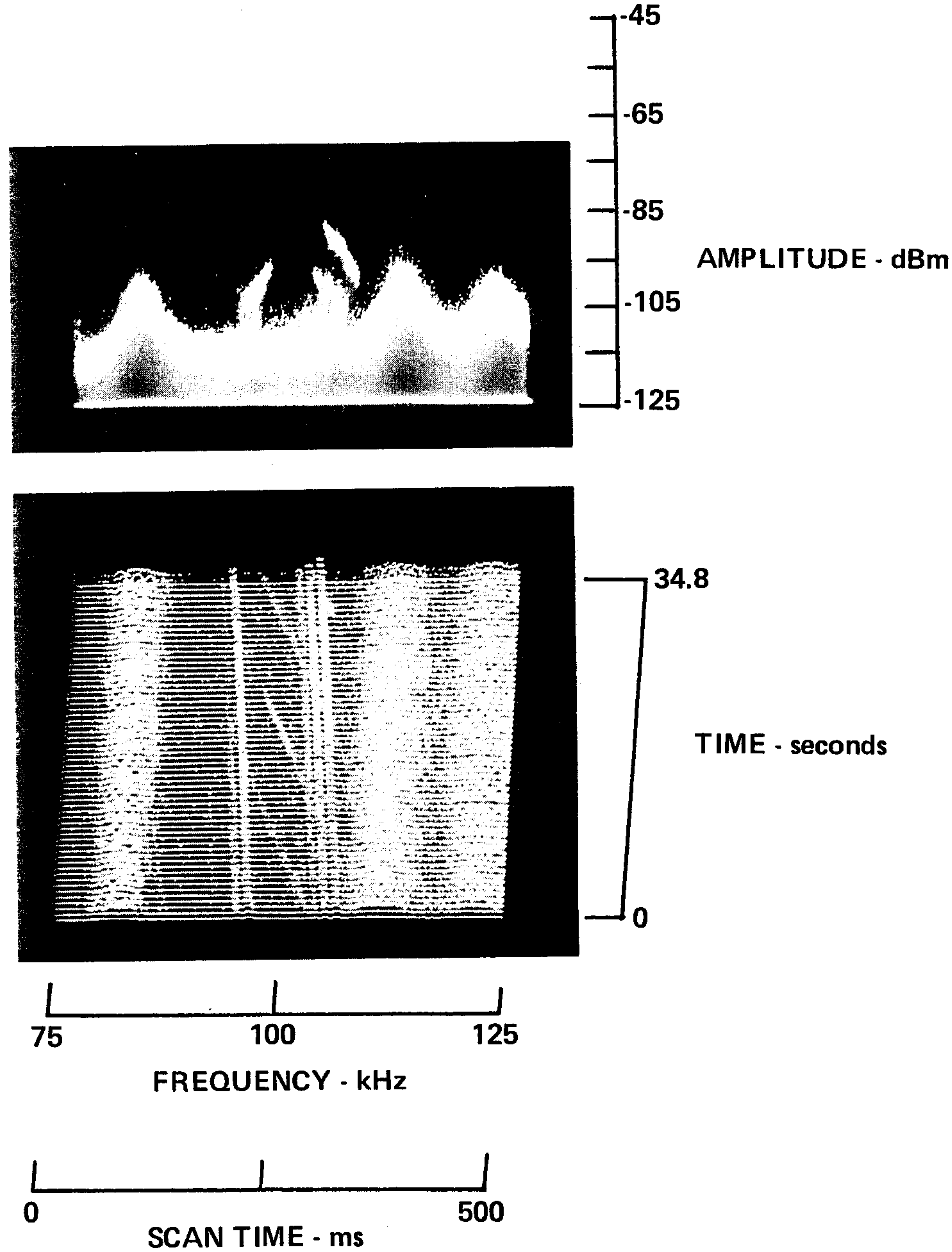

1-22-79, 1334, 106-006
HP140, Whip, F100, W50, IF3, ST 500, A -30/0/+15ΔF

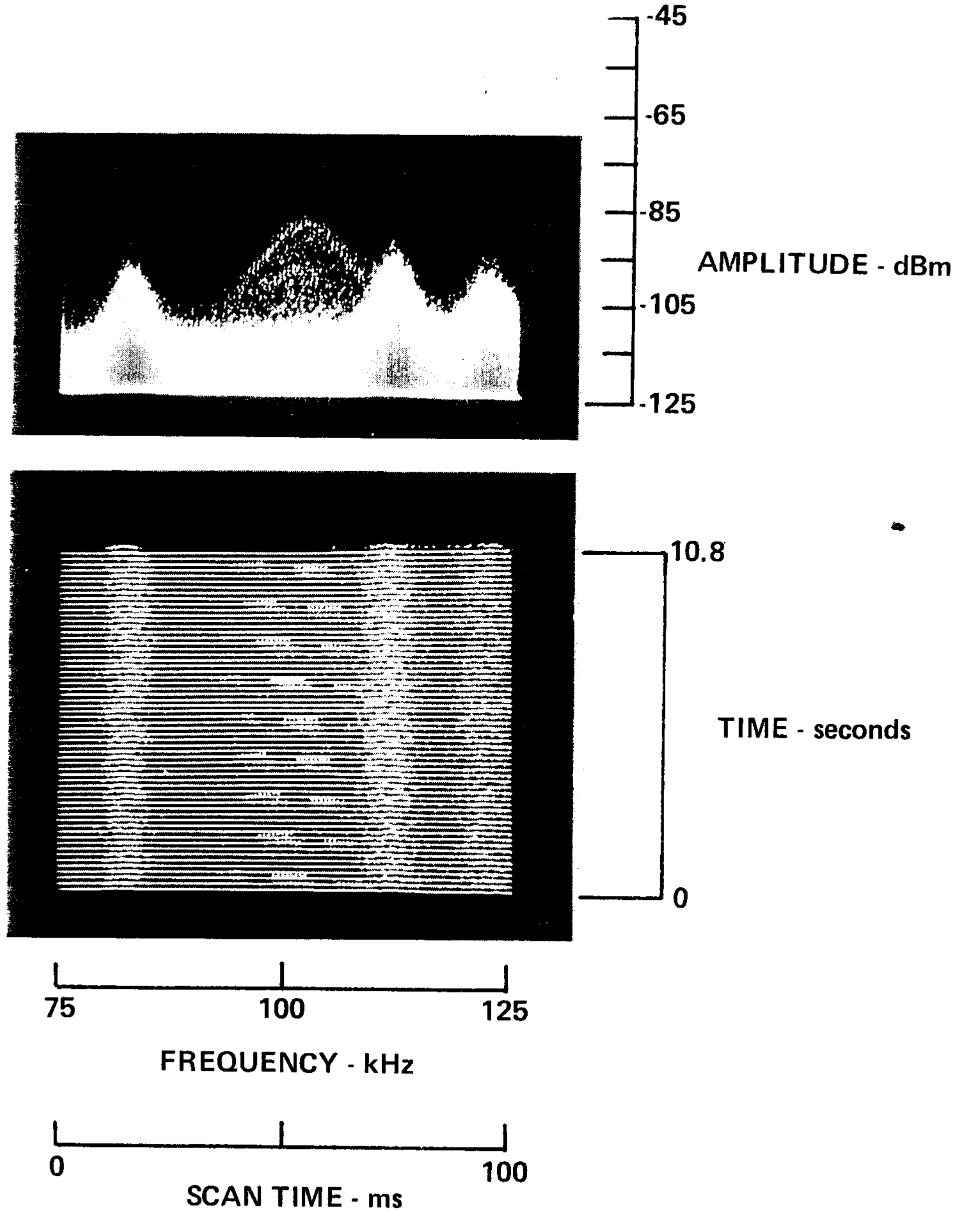

1-22-79, 1036, 106-006
HP140, Whip, F100, W50, IF3, ST 100, A -30/0/+15/NF

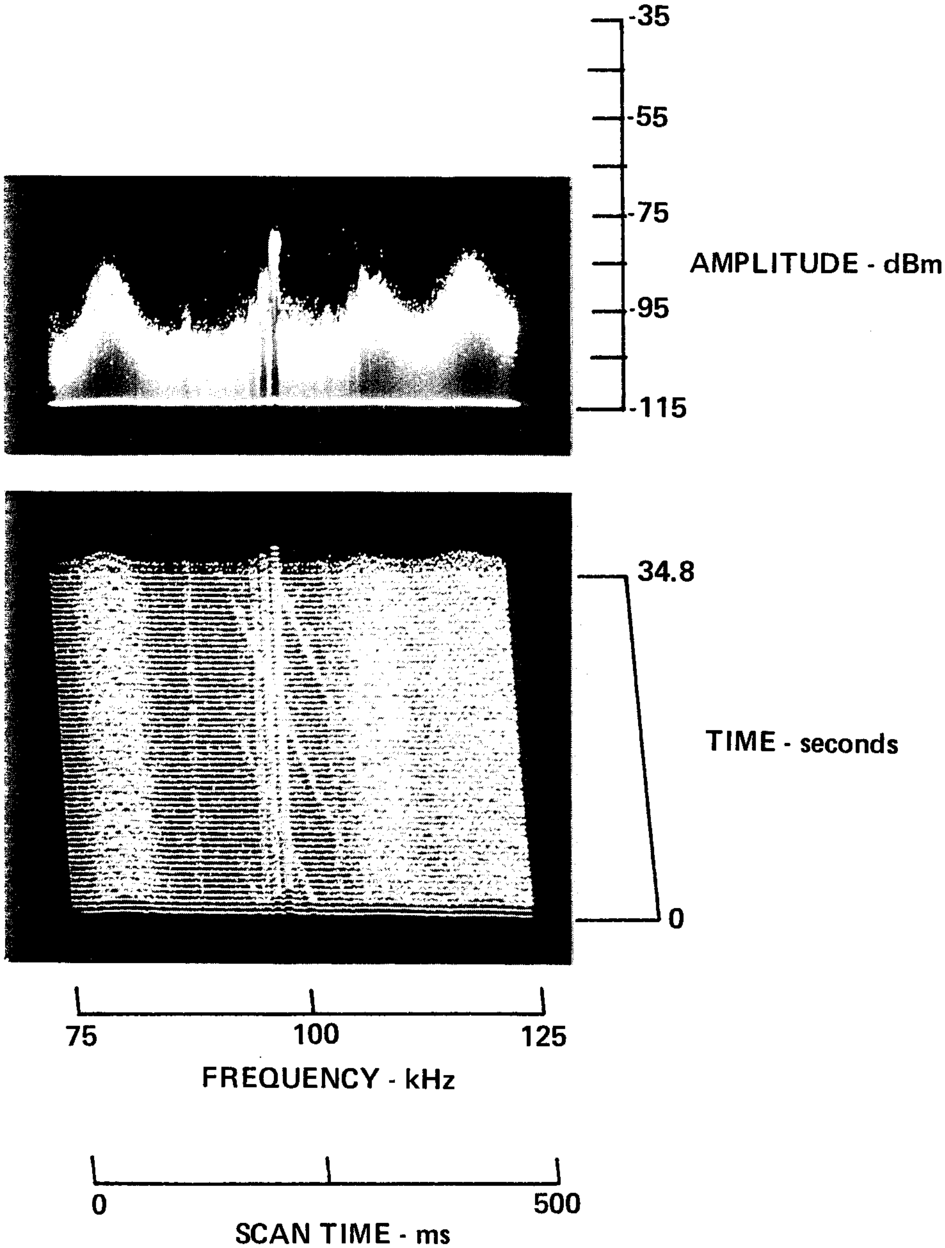

HP140, Whip, F100, W50, IF3, ST 500, A -20/0/+15/NF

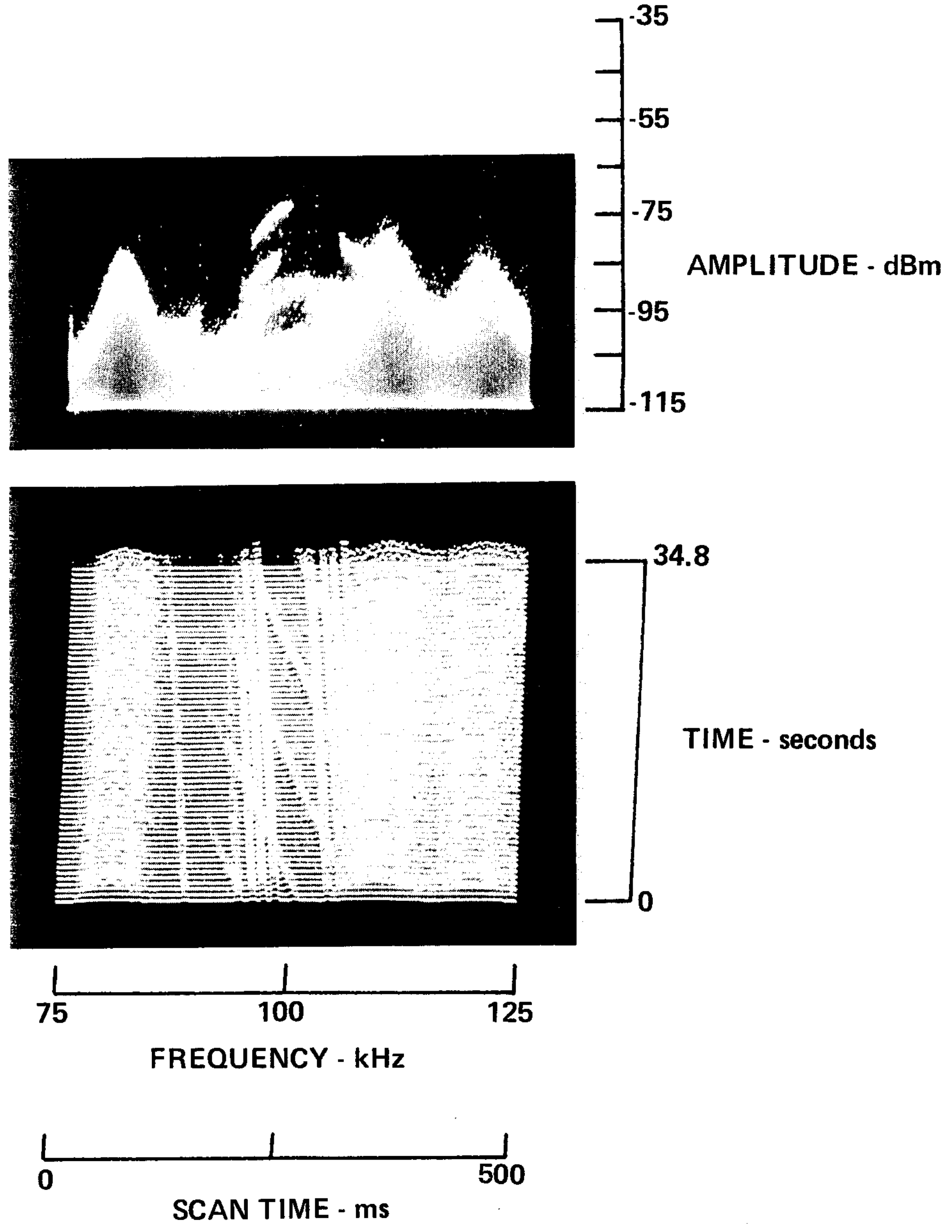

1-22-79, 1142, 106-008
HP140, Whip, F100, W50, IF3, ST 500, A -20/0/+15/NF

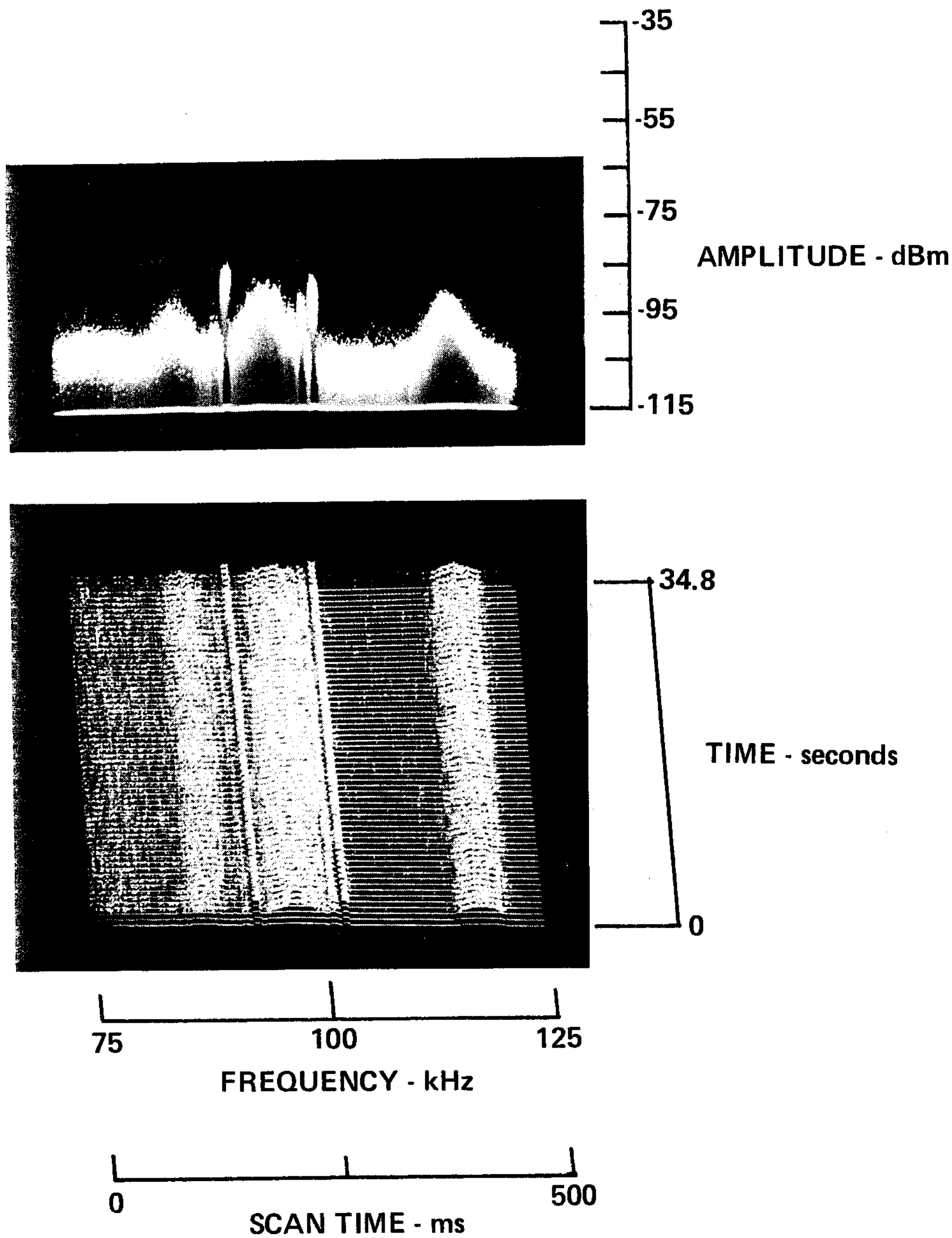

1-22-79, 1159, 106-009
HP140, Whip, F100, W50, IF3, ST 500, A -20/0/+15/NF

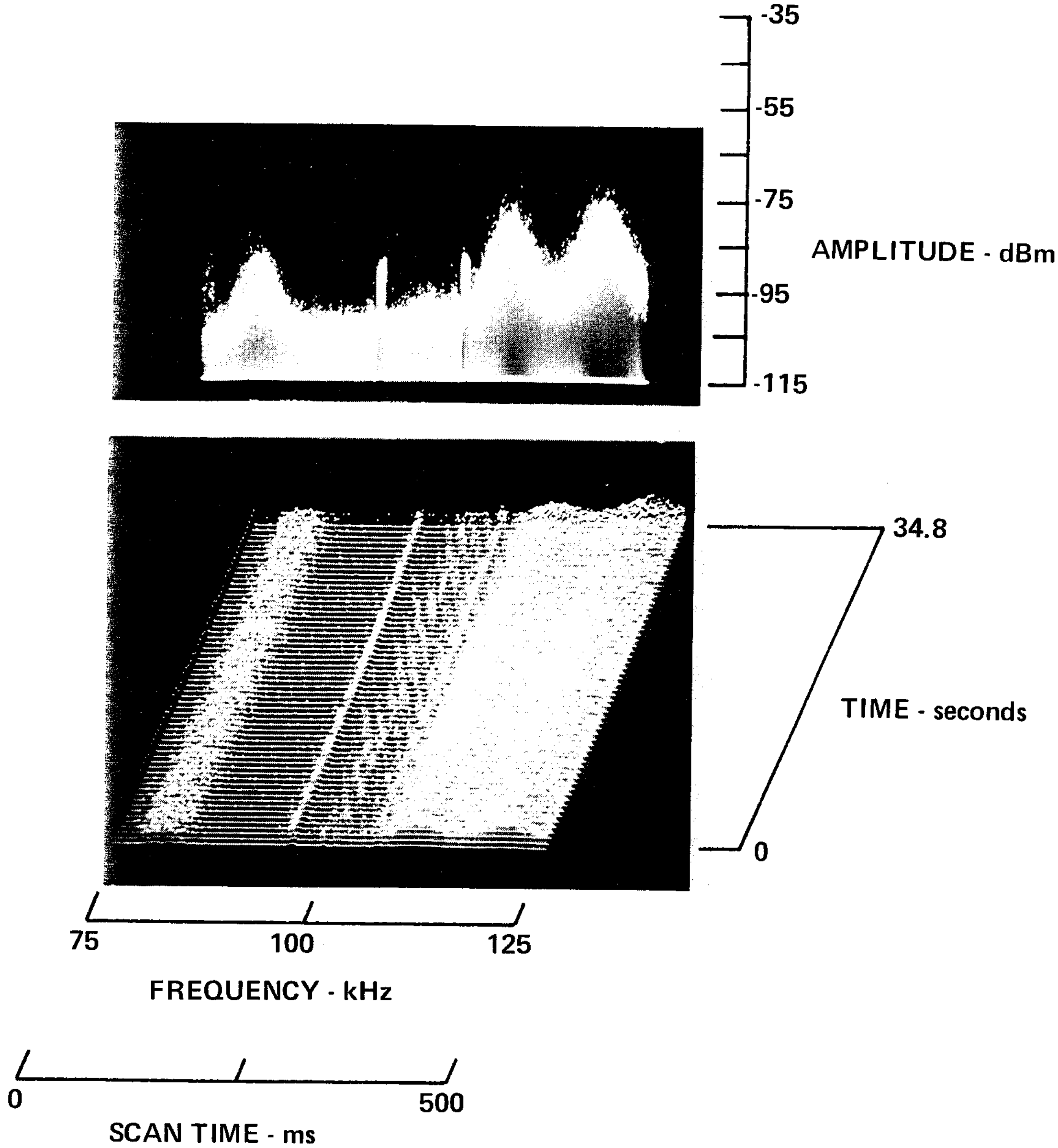

1-22-79, 1222, 106-010
HP140, Whip, F100, W50, IF3, ST 500, A -20/0/+15/NF

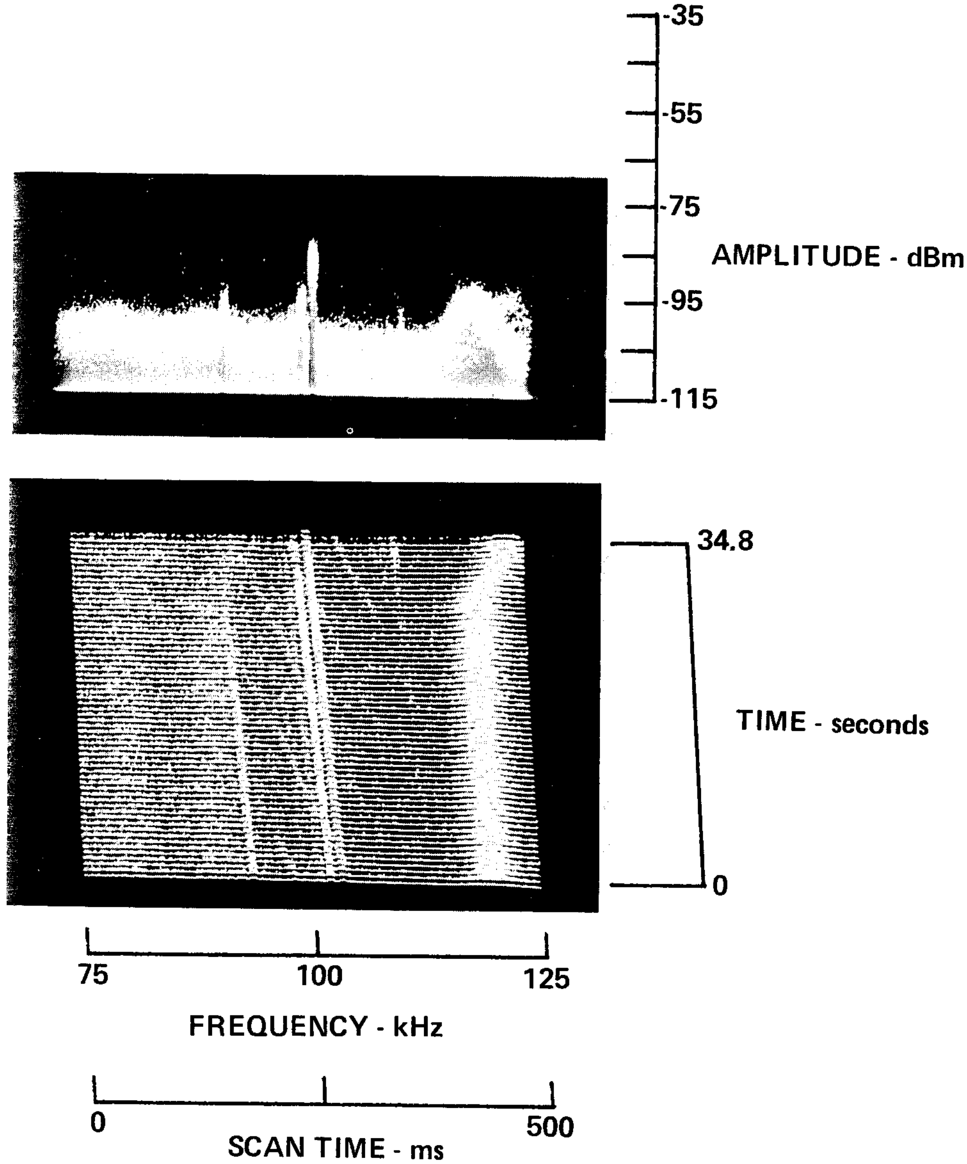

HP140, Whip, F100, W50, IF3, ST 500, A -20/0/+15/NF

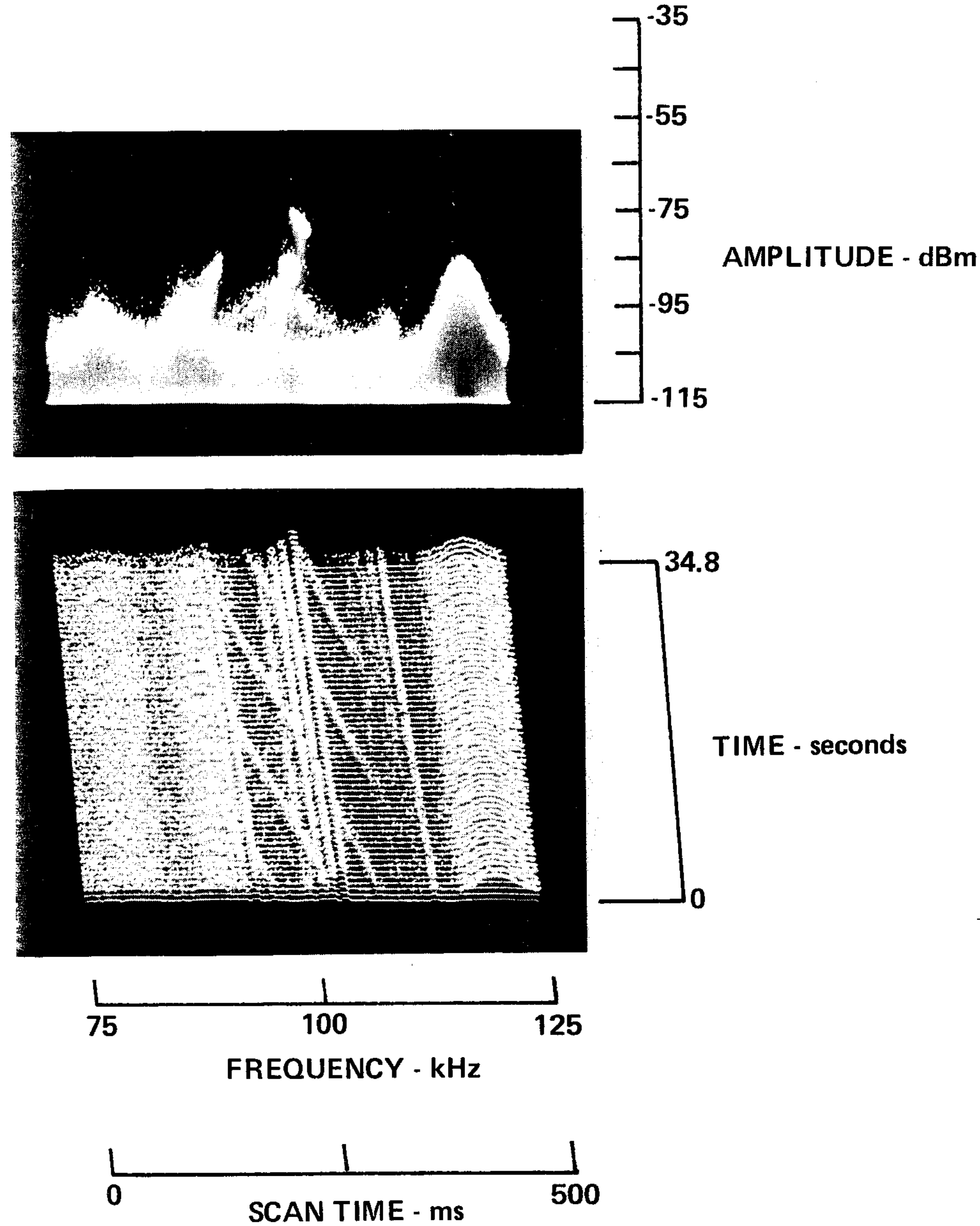

1-22-79, 1304, 109-012
HP140, Whip, F100, W50, IF3, ST 500, A -20/0/+15/NF

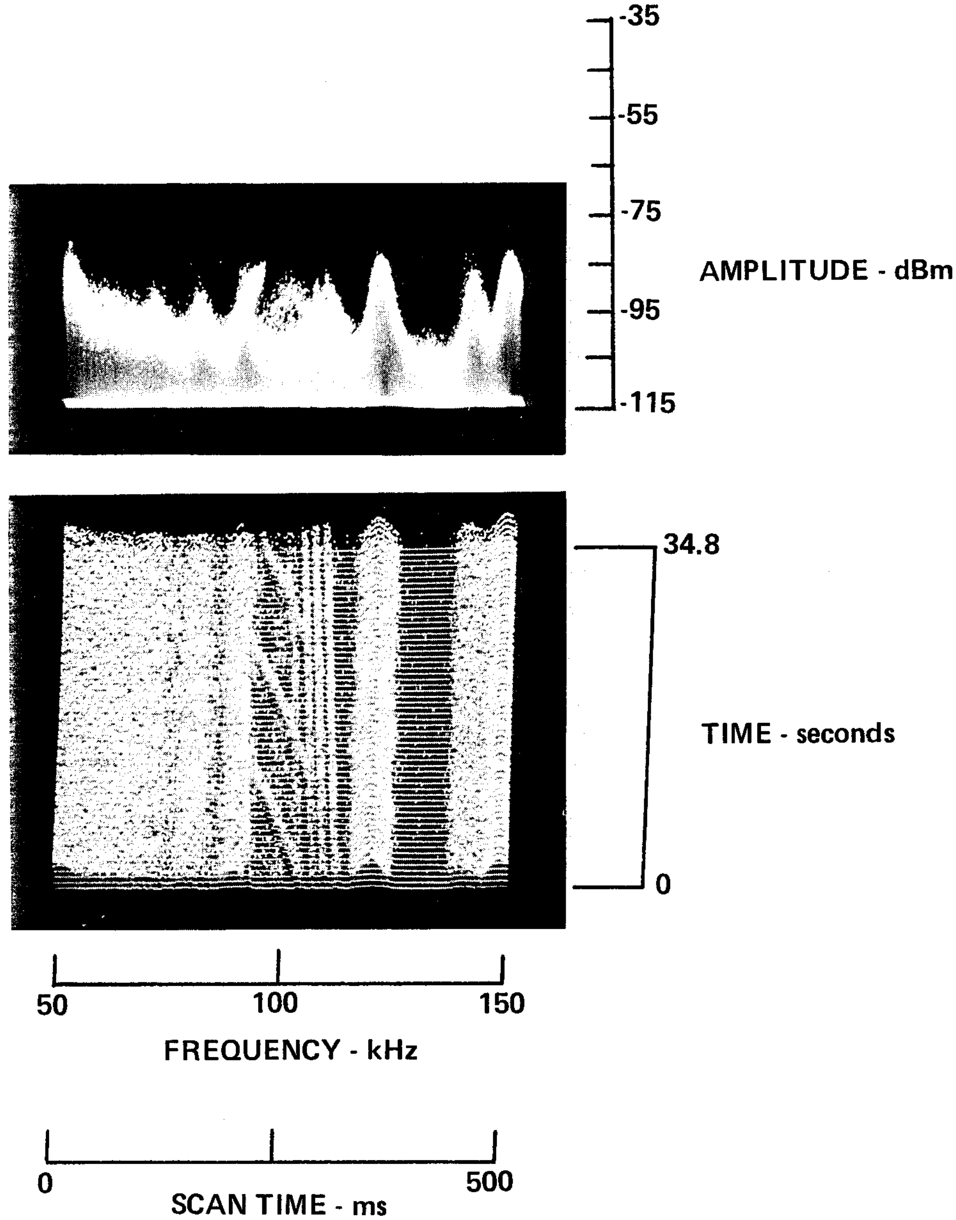

1-22-79, 1307, 109-012
HP140, Whip, F100, W100, IF3, ST 500, A -20/0/+15

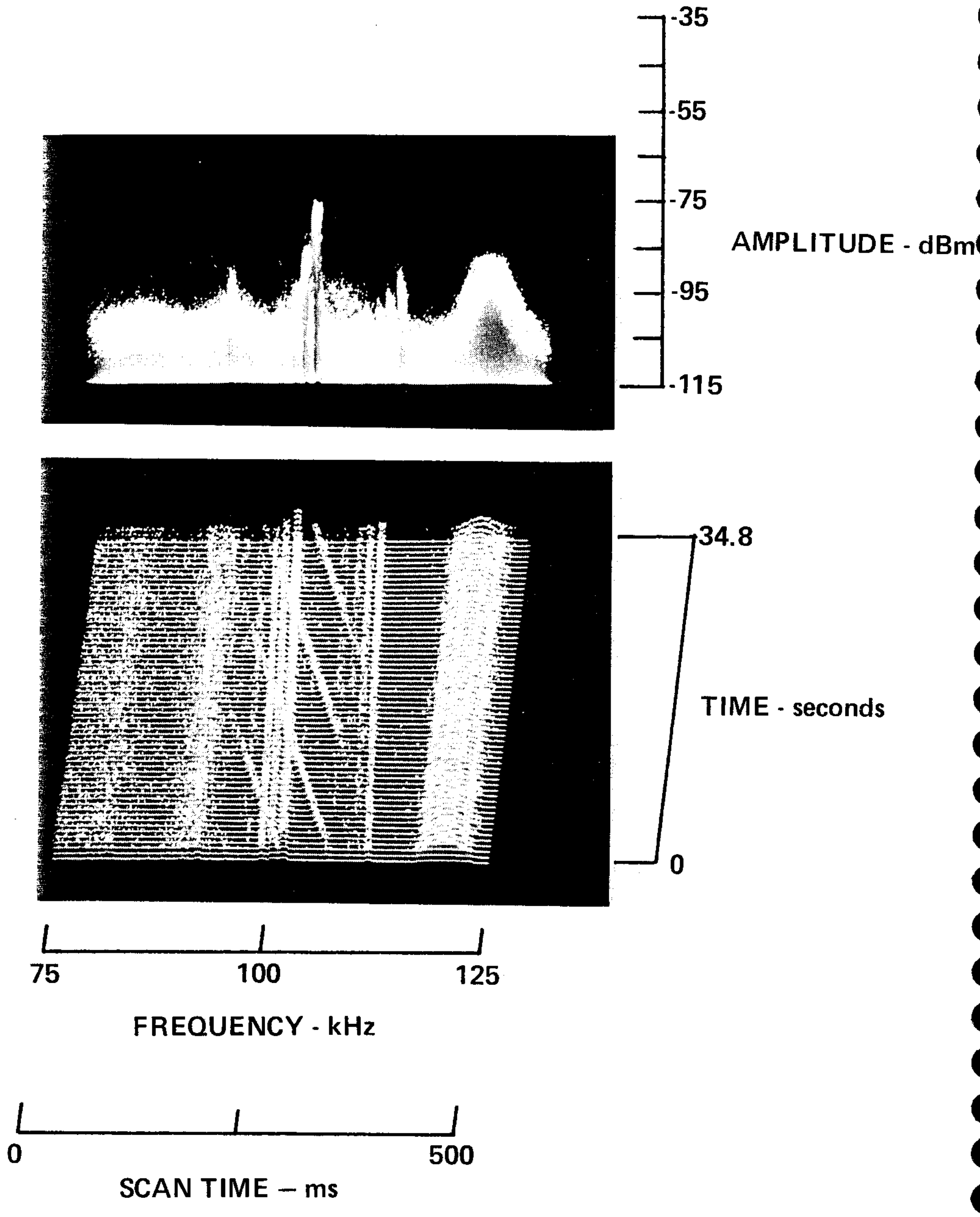

1-22-79, 1320, 109-013
HP 140, Whip, F100, W50, IF3, ST500, A -20/0/+15/NF